Annu. Rev. Astron. Astrophys. 1994. 32: 115–52

PHYSICAL PARAMETERS ALONG THE HUBBLE SEQUENCE

Morton S. Roberts

National Radio Astronomy Observatory[1], Charlottesville, Virginia 22903

Martha P. Haynes

Center for Radiophysics and Space Research and National Astronomy and Ionosphere Center[2], Cornell University, Ithaca, New York 14853, and National Radio Astronomy Observatory, Green Bank, West Virginia 24944

KEY WORDS: galaxies, physical properties, morphological type, mass, star formation

1. INTRODUCTION

One of the remarkable aspects of galaxies is that they can be classified into relatively few categories. The well-ordered sequence of galaxy types appears to offer a clue to possible formation and evolutionary processes. It is thus not surprising that morphology is so frequently an underlying theme in the study of galaxies, and serves as the principal subject of this review. Excellent discussions of recent classification systems are given by Buta (1992a,b). For other reviews with historical references, see de Vaucouleurs (1959) and Sandage (1975).

Hubble (1926, 1936) introduced an early scheme to categorize galaxies; its concepts are still in use. In its simplest form, three basic types are recognized: ellipticals, spirals, and irregulars. Most modern schemes try to employ multiple classification criteria. There are two systems in common use today, both similar in application and notation, and both derived from Hubble's original classification scheme. One is the Hubble system as detailed by Sandage (1961)

[1]The National Radio Astronomy Observatory is operated by Associated Universities, Inc., under a cooperative agreement with the National Science Foundation.

[2]The National Astronomy and Ionosphere Center is operated by Cornell University under a cooperative agreement with the National Science Foundation.

0066–4146/94/0915–0115$05.00

(Sandage & Tammann 1987, Sandage & Bedke 1993). The other system, developed by de Vaucouleurs (1959), adds more descriptive details to the notation and extends Hubble's original spiral sequence beyond Sc. Because the application of this system to over 20,000 galaxies in the Third Reference Catalog of Bright Galaxies (RC3, de Vaucoulers et al 1991) has given it wide usage, it is adopted here. A few percent of all galaxies are unclassifiable. Many of these have unusual morphology because they are interacting systems. For the current purpose of looking for trends among average galaxies, we exclude these peculiar objects from our discussion.

Although the criteria for a type assignment are well recognized, the process is in reality subjective. Rather, we seek to replace qualitative measures with quantitative ones and ultimately to uncover the physics underlying galactic structure. As (we hope) will become evident, various trends do exist, but regardless of the parameters, the dispersion within each type is always large, much more so than errors of measurement. One of these trends, that of color with type, has been long recognized (Hubble 1936). Others, e.g. the H_2 content, are only now being evaluated.

Most recently, numerous authors have attempted to classify galaxies using multivariate analysis of available quantitative measures (Whitmore 1984, Watanabe et al 1985). Such quantitative studies show the existence of two principal categories of galaxy parameters: those that measure the absolute scale (size, luminosity, mass) and those that describe more its form (morphology). Because he undertook his classification scheme at a time when distance estimates were available for only a handful of galaxies, Hubble could not discriminate the scale dimension: that intrinsically bright galaxies are bigger and more massive than faint ones of the same morphology.

With notable exceptions and for obvious reasons the study of galaxies is directed primarily to those listed in catalogs, e.g. the New General Catalog (NGC), the Shapley-Ames Survey and its update (RSA), the Uppsala General Catalogue (UGC), and the various editions of the Reference Catalogues (RC). They are all flux- or diameter-limited. They all suffer from Malmquist bias and they are all deficient in low surface brightness systems. They list the brighter galaxies though generally not the most or least luminous systems. And they mostly contain nearby galaxies, i.e. $z \ll 0.1$. These are systems for which we have the most data, and it is such "catalog galaxies" that we discuss here. We also construct an approximately volume-limited sample; mean values of intrinsic properties, e.g. linear diameter, absolute magnitude, so derived are generally smaller because of Malmquist bias, but show trends with type similar to those for the biased samples.

The ability to measure properties is not equal for all types. Thus HI is rare in elliptical systems, and we lack any meaningful HI parameters for these systems. Similarly, total mass estimates for Es, when available, are based on

different approaches and assumptions than for spirals. For the latter, rotational velocities are derivable from 21 cm HI observations, while the most common kinematic parameter measured for ellipticals is the central velocity dispersion (see Whitmore et al 1985 for a catalog.) Comparison of total mass estimates between Es and spirals are accordingly uncertain and are not made. Other properties such as CO and its derivative, H_2 content, or X-ray luminosity are available only for relatively small samples and suffer accordingly. For X rays, the best that can be done at present is to contrast data for ellipticals with those for the overall spiral category; we note interesting differences.

The most obvious omission is the lack of any distinction between regular and barred spirals. Here we have been guided by Holmberg's (1958) remarks in his classic paper on the photometry of galaxies. He notes:

> . . . that the majority of spiral nebulae exhibit a more or less pronounced bar; the bar may not always be recognizable on the blue plate, but is usually visible on the photovisual exposure. It seems quite possible that a bar is a structural detail common to all, or most, spiral nebulae and that the observed differences are of a quantitative rather than qualitative nature.

This is strikingly illustrated for M51 (Zwicky 1957, Figure 41) by means of a composite of yellow and blue sensitive images. In this composite M51, a classic "regular" spiral shows a small but pronounced bar in its central region.

Some caveats must be emphasized. There are many type-dependent trends to be found in the literature, based on widely ranging sample sizes of various levels of confidence. We are unable to discuss all or even a significant fraction of these. Since our focus is on type-dependencies, other and possibly related issues are treated only briefly. We apologize at the onset if your favorite relationship is omitted and hope that the references will guide the reader to more extensive discussions on these topics.

2. OVERVIEW: THE MORPHOLOGICAL DEPENDENCE OF FUNDAMENTAL PROPERTIES

In an early study of the integral properties of galaxies, Roberts (1969) analyzed 98 spiral and irregular galaxies for which total mass, neutral hydrogen content, luminosity, color, and radius were available. Over the past several decades, the database of observed quantities for extragalactic objects has expanded at an enormous rate. The availability today of large catalogs of galaxies and compilations of data in digital form makes statistical and graphical analysis possible as it has not been before. In preparing this review, we have drawn upon such catalogs to explore several of the morphological-dependence issues.

In this section, we present the results of our own analysis which we discuss in comparison with the findings of others in later sections.

Construction of Samples for Analysis

For the current purpose, we make use of two primary compilations: first, the RC3 and second, a private catalog maintained by R. Giovanelli and M. Haynes that we refer to by its familiar name, the Arecibo General Catalog (AGC). The latter catalog primarily adds a significant body of HI line data including upper limits for non-detected objects, a variety of measurements of the 21 cm line width, and qualitative indicators of profile shape.

Currently, redshift surveys extend relatively deeper in the north than in the south (as visible in Figure 2 of Giovanelli & Haynes 1991). Because of the northern hemisphere bias in redshift survey depth, we use as the prime deep sample the compilation of objects that are included both in the RC3 and in the *Uppsala General Catalogue* (Nilson 1973). We refer to the sample of objects common to both catalogs as the "RC3-UGC sample." It should be noted that, because the RC3 is intended to be complete only for objects of high surface brightness, the lowest surface brightness objects are found only in the UGC, and are underrepresented in the current analysis. Likewise, the UGC, being angular-diameter limited, is biased against high surface brightness, compact objects and becomes incomplete for early-type galaxies especially at the larger distances.

When one selects galaxies of fixed flux, the volume element containing the more distant, intrinsically brighter objects is larger than that occupied by the nearer, intrinsically fainter population. This "Malmquist bias" affects all galaxy catalogs that are flux-limited. In order to examine (and counteract) the effects of Malmquist bias, we have also constructed a nearby volume-limited one that should be complete but has relatively fewer galaxies. Since the volume occupied by the Local Supercluster has been well-studied by most available multiwavelength techniques, we have identified 4972 RC3 objects with redshifts implying membership in the Local Supercluster, i.e. with $V_{\rm LG} < 3000$ km s^{-1}. This subset is referred to as the "RC3-LSc sample." Note that it contains galaxies that are not in the RC3-UGC sample.

Since the backbone of our compilation is the RC3, the reader is referred to its first volume for an explanation of its contents. Our general philosophy has been to use all of the corrected parameters directly from the RC3 when available since its authors have gone to considerable length to reduce parameters obtained from different sources to a standard system. For the present comparative purposes, the consistency of approach is perhaps more critical than absolute prescription. Most parameters as detailed below have been taken directly from the RC3. Additional radial velocities, 21 cm parameters, and far infrared data from *IRAS* come from the AGC.

DISTANCES In order to convert velocities to distances and to further calculate intrinsic parameters, it is necessary to adopt a value of the Hubble constant and a model of the local velocity field. Heliocentric velocities $V_\odot$ are taken from the AGC preferentially if a good quality 21 cm spectrum is available; otherwise, the available optical velocity is used. The velocity with respect to the Local Group V_{LG} was calculated by applying the standard correction to $V_\odot$ given in the RC3: 300 sin$l$ cos$b$. For objects in the Local Supercluster, a nonlinear infall model was used to calculate the distance to an object with the observed V_{LG}. The model adopted follows the outline of Schechter (1980) with the assumptions of a distance of 20.0 Mpc and an overdensity of 2 for Virgo and an infall velocity at the Local Group of 300 km s^{-1}. The Local Supercluster boundary is taken to be at $V_{LG} = 3000$ km s^{-1}. For more distant objects, distance is computed merely from the Hubble ratio using V_{LG} and is not referenced to any other frame. The assumptions that we have made are not intended to be an endorsement of any particular solution but are chosen for convenience. Most important is our emphasis on consistency. Throughout this paper, we adopt a Hubble constant H_o of 50 km s^{-1} Mpc^{-1}.

OPTICAL SIZE, LUMINOSITY, AND SURFACE MAGNITUDE The linear size follows from the RC3 and the calculated distance. Likewise, the prescriptions outlined in the RC3 for correcting magnitudes are adopted along with a value of the solar absolute magnitude M_B of +5.48. The surface magnitude Σ_B used here is defined simply as $\Sigma_B = B_T^0 + 2.5 \log ab$, with a equal to D_{25} and b is the corresponding minor axis obtained from the RC3 axial ratio. Note that the area term here is different from that used below for surface densities.

NEUTRAL HYDROGEN MASS AND SURFACE DENSITY The total neutral hydrogen mass M_{HI} in solar units is calculated from the integrated 21 cm line emission $M_{HI} = 2.36 \times 10^5 D^2 \int SdV$, where D is the distance in Mpc and $\int SdV$ is the HI line flux in Jy km s^{-1}. For objects for which only a value of the rms noise per velocity interval in the emission spectum is available, the upper limit to M_{HI} is calculated assuming the emission is rectangular, of amplitude 1.5 times the rms noise and width equal to that expected for an Sa–Sb galaxy of similar luminosity, properly corrected for inclination. The latter relationship was derived from the detected objects. Objects showing emission confused with other sources or HI in absorption cannot be used properly in the analysis and have been ignored. The HI surface density, σ_{HI}, has been calculated as $M_{HI}/\pi R^2$ where R is the optical linear radius. Although the use of the optical area makes σ_{HI} a hybrid quantity, Hewitt et al (1983) have shown that on average, the HI and optical sizes scale linearly. Most authors use the quantity σ_{HI} or some variant thereof as the indicator of HI content in comparative studies.

FAR INFRARED LUMINOSITY AND SURFACE DENSITY The far infrared luminosity is derived from the fluxes measured by *IRAS* in the 60 and 100 micron bands

$F_{\rm FIR}({\rm Jy}) = 2.58\ F_{60\mu} + F_{100\mu}$, as $L_{\rm FIR}(L_\odot) = 3.86 \times 10^5\ D^2\ F_{\rm FIR}$. Similar to $\sigma_{\rm HI}$, a hybrid far infrared luminosity surface density $\sigma_{\rm FIR}$ is calculated as $L_{\rm FIR}/\pi R^2$.

TOTAL MASS AND SURFACE DENSITY FOR SPIRALS For the galaxies for which 21 cm line emission is detected, profile widths are available to provide an estimate of the circular rotation velocity. Since widths are often measured using different algorithms, we have selected a subset of the available data that meet the following criteria: 1. the level at which the width was measured must be either at 20% of one or more peaks or 50% of the mean intensity; 2. the detection must be a good one, that is, not poor or confused; and 3. the inclination must be greater than 40° for the width to be corrected to edge-on. While these restrictions cut down the number of galaxies for which corrected 21 cm line widths are available, they insure greater certainty of the resultant correlations. The total mass $M_{\rm T}$ determined in this way is available only for non E-type systems, and is calculated according to $M_{\rm T}(< R)\ (M_\odot) = 2.325 \times 10^5 R V_{rot}^2$. As a practical application, we use the corrected 21 cm line width as the measure of $2V_{\rm rot}$ and D_{25} as the indicator of $2R$. Note that we have not applied a correction for turbulent velocity. The total mass surface density $\sigma_{\rm T}$ is likewise calculated as $M_{\rm T}/\pi R^2$.

The Limitations of Galaxy Catalogs

All catalogs have limitations because of the adopted inclusion criteria and their degree of completeness, and conclusions drawn from the examination of any catalog (or data set) must consider those limitations. Of particular importance, as noted by many authors, are biases against low surface brightness objects or the lack of homogenous sky coverage or survey depth. All of these issues are relevant to the current analysis. Given the catalogs from which we have drawn the sample analyzed herein, even before beginning, we want to emphasize the following failings of our analysis:

1. Low surface brightness galaxies, including both the low mass, low luminosity dwarfs and the low surface brightness giants such as Malin 1, are not included in our results.

2. Likewise, compact high surface brightness objects are also excluded. These include both compact BCDs and the smaller galaxies of intermediate luminosity in clusters.

3. Malmquist bias certainly is present in these data. Nearby samples include a predominance of low luminosity, low mass objects that are absent in samples at larger distances. Non-detections of HI and *IRAS* flux provide meaningful upper limits only for nearby samples. This is discussed further below.

4. Types earlier than Sa suffer from a large fraction of non-detections in the 21 cm line measurements. While estimates of the HI mass and surface density can incorporate upper limits to the detected flux (as discussed below), total mass calculations that use the 21 cm line width as a measurement of the rotational velocity cannot be made for non-detections. Hence all discussions of such properties as total mass, mass surface density, and mass-to-light ratio are limited to S0/a–Im. For the Im objects, only the brighter, higher surface brightness members of the class are included; for the S0s only those with HI detections are included.

MALMQUIST BIAS The RC3 is to some degree magnitude-limited, and in most instances, the Malmquist bias seriously affects the availability of data for the present analysis. Figure 1 demonstrates that the Malmquist bias seriously affects the sampling of optical luminosities L_B. The upper panel shows clearly that the low luminosity galaxies are only sampled nearby, becoming increasing absent in samples at larger distances. The figure also demonstrates that there is a maximum luminosity near $\sim 10^{11.5}\ L_\odot$.

The lower panel examines the effect of Malmquist bias on the derived total mass to luminosity ratio M_T/L_B, in logarithmic units. Although this ratio is dependent linearly on distance, there is essentially no distance bias in this ratio.

In the following section, we present the analysis of both the RC3-UGC and RC3-LSc samples separately in order that we might keep the effect of Malmquist bias in perspective in interpreting our results.

Summary of Results

Given the available data, we are able to calculate the following properties: linear radius R_{lin}, blue luminosity L_B, far infrared luminosity L_{FIR}, total mass M_T, neutral hydrogen mass M_{HI}, the ratios M_T/L_B, M_{HI}/L_B and M_{HI}/M_T, the blue surface magnitude Σ_B, and the surface densities Σ_T, σ_{HI}, and σ_{FIR}. Figures 2–4 summarize our examination of morphological dependence in the fundamental properties for both the RC3-UGC (circles) and RC3-LSc (squares) samples as described above. In each panel, the median (filled symbol) and mean (open symbol) values for each morphological class are plotted along with an indication of the interquartile range (vertical bar extending from the values at the 25th and 75th percentiles). Although in most cases the median and mean values are not significantly different, many of the distributions are significantly non-Gaussian and sufficiently broad and skewed that the mean value is not a useful indicator. In settling on this presentation, we have also examined histograms of each distribution. Note that, although a logarithmic scale is used in the display, all quantities have been calculated using linear variables where logarithms are not already involved (e.g. B-V). Where necessary, survival analysis has been applied in the calculation of mean values but it should be

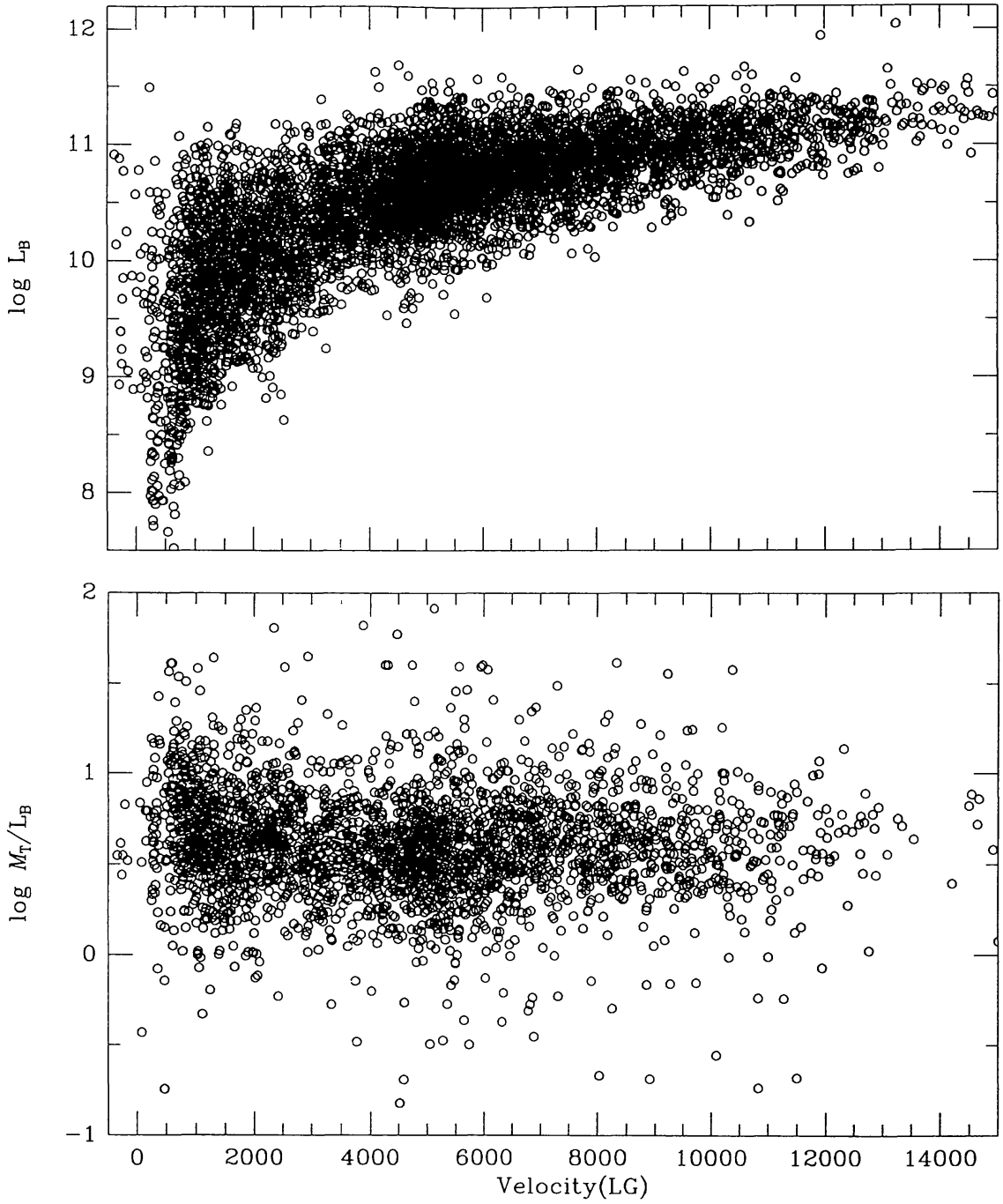

Figure 1 (*Upper*) Blue luminosity vs corrected velocity. The data representing 7930 galaxies in the RC3-UGC sample clearly illustrate the Malmquist bias. (*Lower*) The total mass-to-luminosity ratio for 2864 galaxies in the RC3-UGC sample vs velocity. This ratio has a distance term but the data show essentially no distance or Malmquist bias.

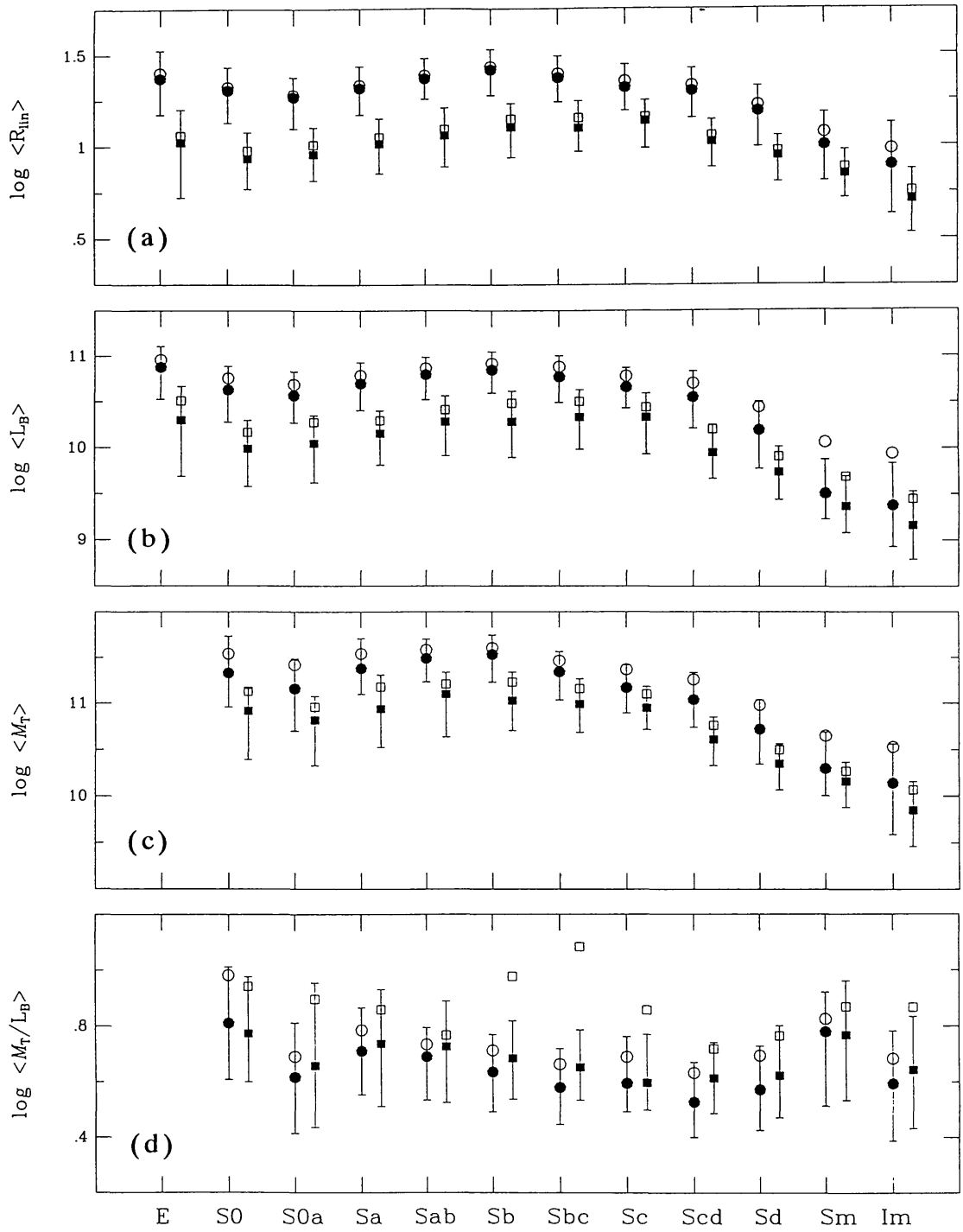

Figure 2 Global galaxy parameters vs morphological type. Circles represent the RC3-UGC sample; squares the RC3-LSc sample. Filled symbols are medians; open ones are mean values. The lower bar is the 25^{th} percentile; the upper the 75^{th} percentile. Their range measures half the sample. The sample size is given in Table 1. (*a*) log linear radius R_{lin}(kpc) to an isophote of 25 B mag/arcsec^2 , (*b*) log blue luminosity L_B in solar units, (*c*) log total mass M_T in solar units, (*d*) log total mass-to-luminosity ratio M_T/L_B.

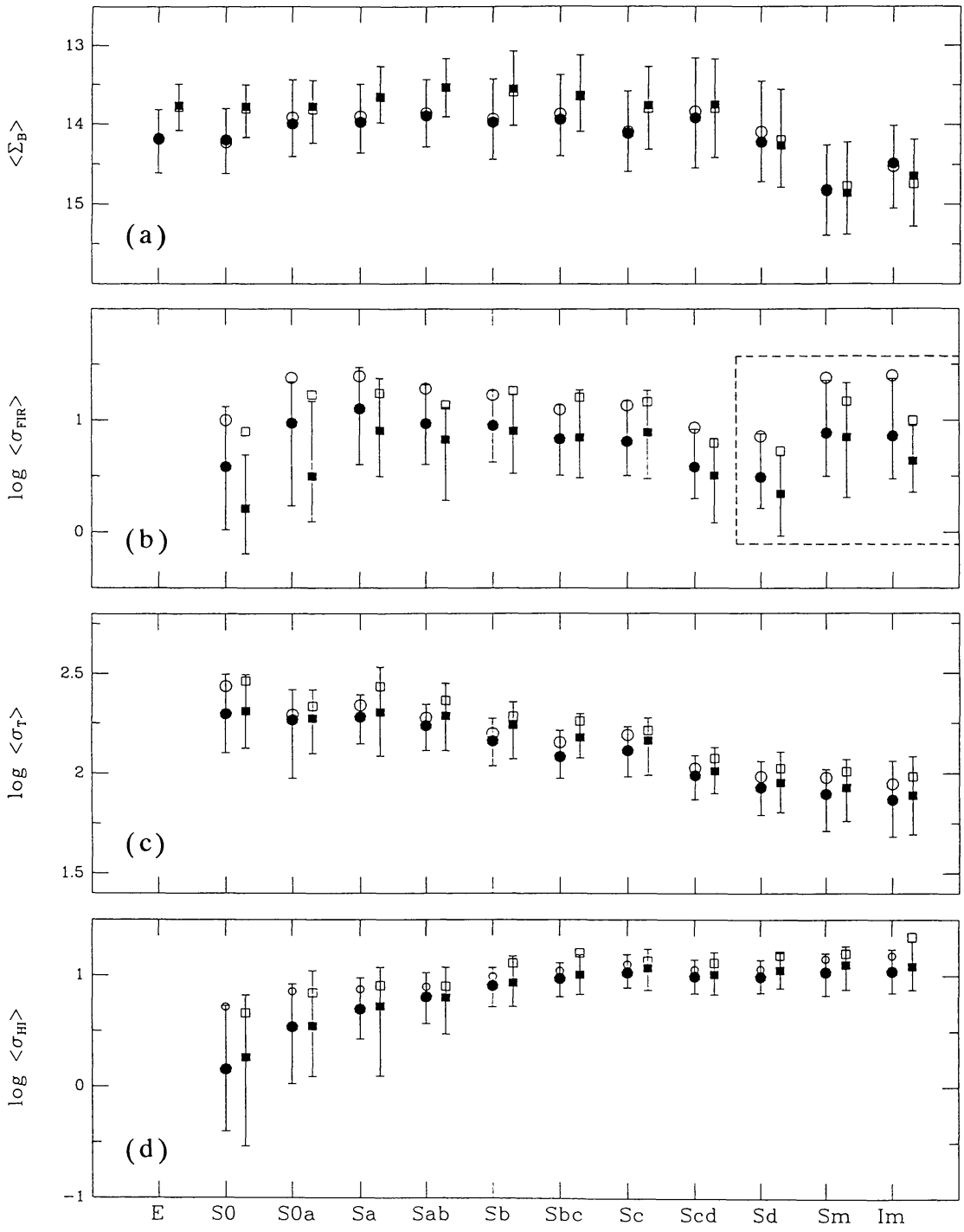

Figure 3 Same as Figure 2, for (*a*) optical (blue) surface brightness Σ_B, (*b*) log FIR surface density σ_{FIR}, (*c*) log total mass surface density Σ_T, (*d*) log HI surface density σ_{HI}. Dashed lines delineate the types with significantly fewer data.

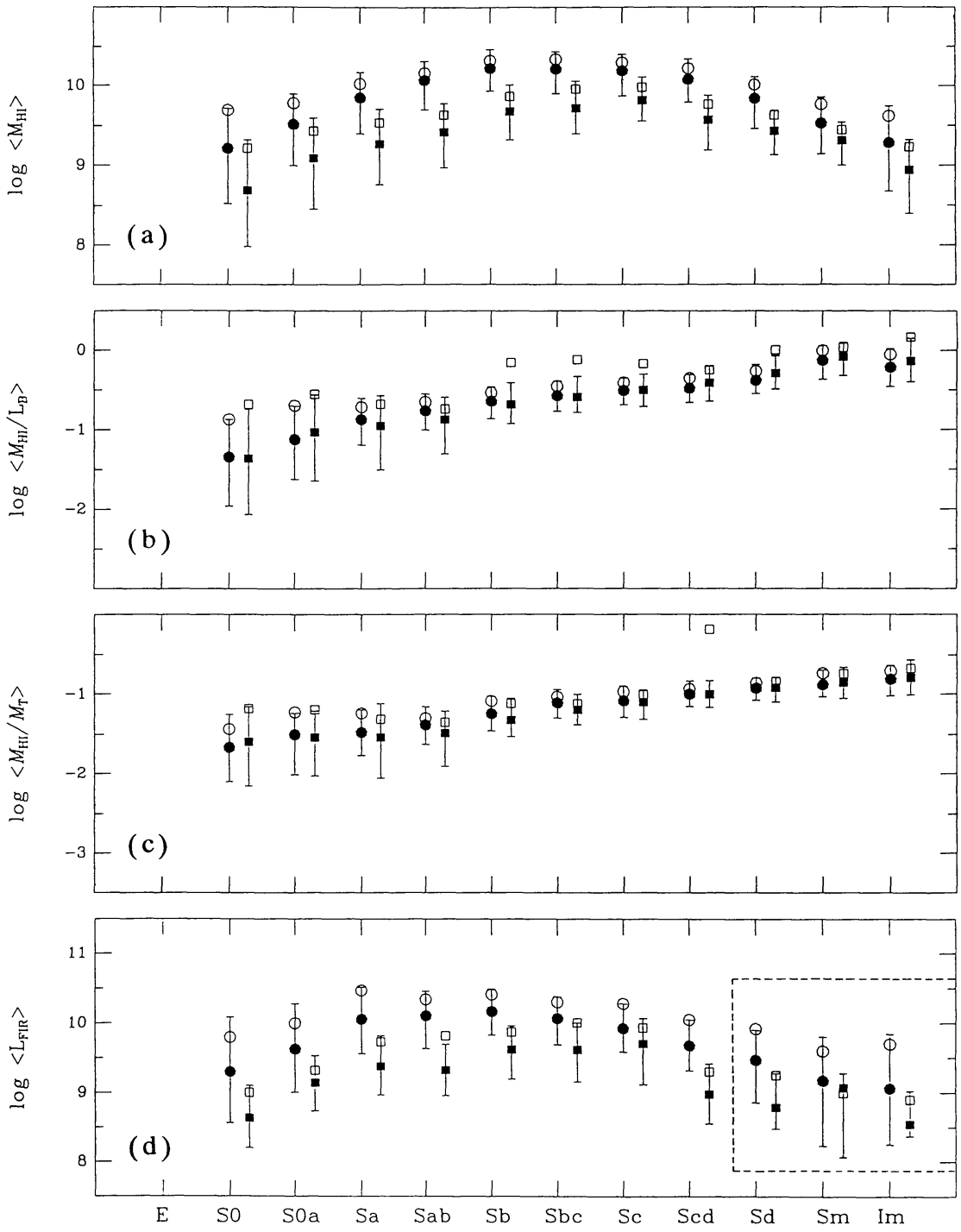

Figure 4 Same as Figure 2, for (*a*) log total HI mass M_{HI}, (*b*) log HI mass-to-blue luminosity ratio M_{HI}/L_B, (*c*) log HI mass fraction M_{HI}/M_T, (*d*) log FIR luminosity L_{FIR}. The dashed lines indicate significantly fewer data for these types.

noted that medians and percentiles treat non-detections as detections. Median and quartile values, along with the number of galaxies in each subsample, are also presented in Table 1 (see the end of this chapter). Since we note that for many properties there is little variation over adjacent types, pairs of morphological classes are combined in producing the table in order to shorten the presentation.

It is convenient to adopt Binggeli's (1993) nomenclature for giant "classical" and dwarf systems. He refers to spirals of type Sa, Sb, and some Scs as "classical spirals" with the term "dwarf irregulars" applying to types Sd, Sm, and Im as well as late Scs. This is not only useful for descriptive purposes but, as evident in the figures and Table 1, marks an important dividing line in certain of the global properties of galaxies.

In the next sections, we use these graphical and tabular summaries in the discussion of the properties of the normal galaxy population.

3. DISCUSSION OF GALAXY PROPERTIES

As mentioned in the introduction, the classification of galaxies by morphological appearance and the variation in scale properties within a single class are the primary discriminants among galaxies. Here we review the individual properties available from large surveys and attempt to identify the variations that relate more to form than to scale.

Optical Colors

A classic study of galaxies was done by Holmberg (1958) who compiled and analyzed photometric data (integrated magnitudes, colors, and diameters) for 300 galaxies. One of his main conclusions was the dependence of color on morphological type. Objects of different morphological classes show clear differences in their optical colors as measured by the color indices $(U-B)$ and $(B-V)$. Figure 5 shows the well-established trend between morphology and mean color. The E and S0 galaxies are clearly redder than their spiral counterparts, and the trend from redder to bluer is nearly monotonic. At the same time, the range of colors among the Sa galaxies overlaps that of Sc galaxies: some Scs are as red as some Sas while some Sas are as blue as some Scs. It is unlikely that this overlap results from misclassification or observational errors, but rather that the scatter reflects true variations in the colors, and presumably the current star-formation rates, in individual objects.

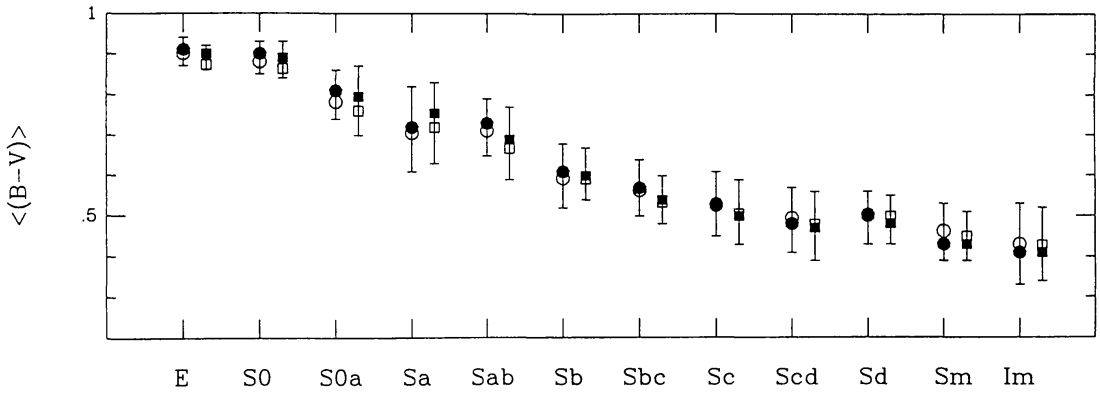

Figure 5 (B – V) color vs morphological type. (Same symbols as in Figure 2.)

Optical Linear Size

Both the median and mean values of linear diameter show subtle differences along the Hubble sequence as evident in Figure 2*a*, with the most distinguishing feature being the "smallness" of the latest types. Within the RC3-LSc sample, the classical spirals show a small systematic increase in size toward the later types. Such a trend is less obvious in the flux-limited RC3-UGC sample. The largest early-type galaxies, the cDs, are underrepresented in the current sample since they are too rare to be found nearby. Their location in regions of highest local density suggests that their large sizes are related to their spatial locations in the deepest potential wells.

It should be noted that the Malmquist bias also affects diameter-limited catalogs in the sense that objects at larger distances have characteristically larger linear diameters. The measurement of optical size enters into the debate concerning the degree of extinction internal to a spiral disk and into the surface brightness level to which a diameter measurement refers (Valentijn 1991, Burstein et al 1991, Giovanelli et al 1994).

Optical Luminosity

The optical luminosity L_B is a parameter of scale. Like the linear size, the range of median L_B values characteristic of classical galaxies varies only slightly, until the latest types, where the distinctiveness of the dwarfs becomes evident (Figure 2*b*). The ellipticals here are slightly brighter than spirals.

LUMINOSITY FUNCTION Binggeli et al (1988) have carefully reviewed what is currently known about the luminosity function $\Phi(L)$. In their study of the Virgo cluster (Binggeli et al 1985), they derive the luminosity function $\Phi(L, T)$ for each morphological type separately. The range of luminosities representative of the classical galaxies is seen to be similar, as in Figure 2*b*, with

the later spirals and dwarfs showing a characteristic decrease and being clearly separate. Binggeli et al find that while the brightest galaxies are ellipticals, the most common galaxies are the dEs. Because of morphological segregation, they conclude that $\Phi(L, T)$ cannot be universal. We discuss the effects of morphological segregation in Section 4.

Optical Surface Brightness

Holmberg's survey (1958) included photometric parameters for both magnitude and diameter with which he investigated the surface brightnesses of galaxies and studied the effects of internal extinction. Because internal extinction causes a sytematic change in the observed surface brightness (and color) as a function of inclination, we adopt a definition of surface magnitude that attempts to account for extinction. As mentioned above, the issues of internal extinction are still under significant debate (Disney et al 1989, Byun 1993).

Figure 3*a* shows the global surface brightness within D_{25}, Σ_B. The distribution of Σ_B is nearly constant for the E, S0, and classical spiral galaxies, but distinguishes clearly the late dwarf categories Sm and Im. We emphasize again that, as Disney & Phillipps (1983) discussed, current catalogs are biased against systems of low surface brightness, and some of the relative constancy found here across most of the classical galaxy sequence may be due to catalog selection.

DISK SURFACE BRIGHTNESS AND SCALE LENGTH By examining the available surface photometry, Freeman (1970) found that the face-on central surface brightnesses of most spiral disks are nearly constant, with small scatter: 21.67 $\pm$ 0.30 B-mag arcsec^{-2}. Deviations occur at the ends of the spiral sequence among the S0s on the one side and dwarfs on the other. Surprisingly, most Es also seem to have constant central surface brightness. With the caveat that current catalogs are indeed biased against the low surface brightness systems, most E, S0, and classical spiral galaxies have the same scale length as a function of luminosity regardless of morphology. A thorough discussion of the details of this issue, including the effects of selection bias, is presented in Gilmore et al (1990).

Far Infrared Emission

The *IRAS* all-sky survey has provided measurements, or their upper limits, of the far infrared (FIR) flux in the 12, 25, 60, and 100μ bands. FIR flux measurements of normal galaxies show a clear distinction between elliptical and spiral galaxies. Ellipticals have a much poorer detection rate and when detected are generally lower in both FIR luminosity and in the ratio L_{FIR}/L_B (de Jong et al 1984, Bothun et al 1989, Sauvage & Thuan 1993). Exceptions are found in those early-type systems experiencing starbursts, e.g. NGC 1275 and NGC 1316.

The type dependences of FIR surface density σ_{FIR} and luminosity L_{FIR} are illustrated in Figs 3*b* and 4*d*. Many of the discussions in the literature focus on FIR-bright systems. These tend to be prominent starburst galaxies (e.g. M82), often peculiar in their morphological appearance and/or clearly involved in interaction with another system (Sanders et al 1987, but see Haynes & Herter 1988; Kennicutt 1990). In this review we avoid discussion of such galaxies.

Three possible origins of this FIR radiation are commonly identified:

1. Dust heated by nearby young, massive stars and reradiating in the infrared. The dust-molecular cloud complexes in the plane of the Milky Way are an example.

2. Dust reradiating the heating by the general interstellar radiation field, e.g. the Galactic cirrus cloud population.

3. Thermal and/or nonthermal radiation from active galactic nuclear regions, e.g. Seyfert galaxies.

Reviews of IR and FIR radiation are given by Soifer et al (1987), Telesco (1988), Cox & Mezger (1989), Rowan-Robinson (1990).

If the massive-star population, i.e. O-B stars, are the dominant dust-heating source then the FIR is a good measure of star formation (Devereux & Young 1991, 1992). The cirrus clouds in our Galaxy as well as the obvious presence of a general stellar radiation field have given rise to a two-component model to describe a galaxy's FIR radiation (e.g. Lonsdale Persson & Helou 1987, Buat & Deharveng 1988) with proponents supporting the importance of one model over the other.

In a study of the luminosity ratio $L_{FIR}/L_{H\alpha}$, Sauvage & Thuan (1992) find a systematic decrease from early- to late-type spirals and propose that the cirrus fraction responsible for the FIR luminosity decreases from ~86% for Sas to ~3% for Sdms—a result which would require a large, systematic, type-related correction to the use of L_{FIR} as a measure of star formation. They call attention to an alternative explanation for the $L_{FIR}/L_{H\alpha}$ type correlation: that the initial mass function (IMF) changes with type. They are reluctant to accept this possibility because of the proposal of a "universal IMF" (Scalo 1986), although there are many instances in our own Galaxy of differing IMFs (Gilmore & Roberts 1988). As noted in the discussion on HII regions, there is a strong dependence of number and luminosity of HII regions with galaxy type. This increase in both number and luminosity of HII regions with later type implies a type dependence of the IMF (Kennicutt 1988, 1989; Kennicutt et al 1989) similiar to that suggested above.

The strong correlation of FIR and radio radiation for spirals is difficult to explain in a model that does not invoke massive stars as a heating mechanism (Xu 1990; but see Devereux & Eales 1989). This interpretation does not appear

to hold for normal elliptical galaxies where no FIR-radio correlation is found (Bregman et al 1992). Though visible patches of dust are frequently found in elliptical galaxies, here again there is no correlation with FIR radiation, and the evaluation of the amount of dust in elliptical galaxies from their (weak) FIR luminosity is at best uncertain.

The type dependence of the 1. FIR detection rate, 2. FIR luminosity, and 3. the luminosity ratio FIR/Radio (Fabbiano et al 1988, Condon et al 1991) is most impressive in separating ellipticals from spirals, with S0s somewhat intermediate in these various quantities. As illustrated in Figure 3*b*, the distinction in the FIR surface density within the spiral classes Sa–Sc, if present at all, is only slight (Bothun et al 1989, Sauvage & Thuan 1993).

Radio Continuum Emission

The radio radiation from galaxies generally has two spatial components: 1. that within a nuclear or central region where there may also be various levels of substructure, e.g. jets and knots, and 2. a more extended region, where again there may be structure. One or the other component may be very weak or absent (to the current levels of detection). The literature on radio radiation from normal galaxies is extensive; for reviews see Condon (1992) and Hummel (1990).

There are two basic mechanisms responsible for the radio continuum radiation in normal galaxies: synchrotron radiation arising from relativistic electrons accelerated by supernova remnants, and free-free radiation primarily from HII regions. A third origin due to dust heated by starlight is significant only at wavelengths < 1 mm. Because this review is intended to discuss typical galaxies, we omit consideration of "radio galaxies," i.e. radio-loud systems having radio luminosities $> 10^{33}$ watts (e.g. Virgo A, Cygnus A).

Most normal galaxies are, at best, weak radio sources, and the statistics concerning their radio properties can be correspondingly poor. Thus we note that many of the nearer radio-loud galaxies are of early type, although most early-type galaxies are of very low radio luminosity. Frequently, only upper limits to the radio flux are available.

The early-type galaxies, the Es and S0s, clearly differ from the later-type systems in that compact core sources are common in the former. Extended sources comparable to the visible disk are much more common in the later types. When extended sources are found in the early-type galaxies, they are narrow and suggest jet-shaped sources (Hummel et al 1984, Condon & Broderick 1988, Condon et al 1991).

Another strong distinction between ellipticals and later-type systems is found in the comparison of radio emission with FIR. These two quantities correlate remarkably well for spirals but not for elliptical galaxies and only poorly for S0s (Bregman et al 1992). This holds over a radio frequency range from at least 151 MHz (Fitt et al 1988) to 4.85 GHz (Condon et al 1991) for galaxy types Sa–Im

(Sauvage & Thuan 1993). The proposal here is that the infrared measures primarily the reradiation from dust located near sites of active star formation while the radio measures primarily synchrotron radiation from electrons accelerated by supernova remnants resulting from this active massive star formation.

X-Ray Emission

Most of our understanding of the X-ray properties of galaxies comes from the results of *Einstein Observatory* measurements in the 0.2–3.5 keV X-ray band. Fabbiano (1989) provides a detailed review of X rays from normal galaxies; Sarazin (1992) gives a briefer summary. Catalogs include those by Fabbiano et al (1992) and Roberts et al (1991). *ROSAT* data and reports are appearing as this review is being written. In the near future we can expect important extensions to our knowledge of X-ray sources.

X rays have been detected from all galaxy types except the low luminosity dE and dS0 classes. *ROSAT* detections of X rays in the direction of such dwarfs appear to be background sources (e.g. Gizis et al 1993). There is a correspondence between optical and X-ray luminosities such that only the nearest Im-type systems, those in the Local Group, have thus far been seen in X rays. The optical (blue)-X-ray luminosity ratio differs with galaxy type. Es and S0s have, with large dispersion, an X-ray luminosity that varies approximately as the square of their optical luminosity (Canizares et al 1987, Bregman et al 1992). In contrast, the late-type galaxies show, again with large dispersion, a linear dependence between these two quantities (Fabbiano et al 1988).

Here we limit our discussion to normal galaxies, which have X-ray luminosities in the range 10^{38}–10^{42} ergs s^{-1}. The X-ray spectrum differs with galaxy type, and is harder for spirals. There are two distinctly different origins of the (non-nuclear) radiation: (*a*) a component which is basically stellar in origin: supernova remnants and X-ray binaries, and (*b*) diffuse emission from hot (10^6–10^7 K) gas.

In spirals, the stellar constituent can have both Population I and II components: for the former, supernova remnants and high mass X-ray binaries; for Population II, the so-called low-mass X-ray binaries. In our Galaxy, low-mass binaries are found primarily in globular clusters and in the central bulge region, although some have also been identified in the disk. The million degree gas is the principal source of X rays in the luminous early-type galaxies. This thermal plasma has its origin in the mass lost by evolving stars, stars which in the bulge component of early-type systems have random motions of typically a few hundred km s^{-1}. Ejecta from these evolving stars collide at velocities corresponding to the observed X-ray temperature. Such a source for the X rays so prominently emitted by ellipticals solves the long-recognized dilemma of locating the mass lost during the evolution of these stellar-rich systems.

In summary, X rays are seen from all galaxy types with the properties of

radiation dependent on the fraction of the Population types in each galaxy. This variation is exemplified by bright ellipticals with relatively high luminosity soft X rays and by the bright, late-type spirals with lower luminosity, harder X radiation. The Sas with prominent bulges as well as star-forming disks have X-ray characteristics between those of Es and the later spirals.

Neutral Hydrogen Mass and Content

Because of the sensitivity available at centimeter wavelengths, the 21 cm line has been a valuable tool in measuring the redshifts of galaxies and serves as a general indicator of HI content. Since HI line fluxes, or upper limits, are available for some 15,000 galaxies skywide, the HI content surpasses nearly all other quantitative indicators of the potential for star formation. The HI content of galaxies has been the subject of recent reviews by Haynes et al (1984) and Giovanelli & Haynes (1990). Here we focus only on the morphological dependence among normal objects.

Several quantities are generally used in analyzing the total HI content of galaxies: the total HI mass $M_{\rm HI}$, the hydrogen mass to luminosity ratio $M_{\rm HI}/L_{\rm B}$, and the HI surface density, $\sigma_{\rm HI}$. While both $M_{\rm HI}/L_{\rm B}$ and $\sigma_{\rm HI}$ have been used as the comparative measure of HI content, a residual dependence of the former ratio on $L_{\rm B}$ exists, in the sense that higher luminosity galaxies have systematically lower values of $M_{\rm HI}/L_{\rm B}$. Numerous authors (e.g. Bottinelli & Gouguenheim 1974) have shown that caution is necessary in using $M_{\rm HI}/L_{\rm B}$ if the Malmquist bias might play a role. Furthermore, since $L_{\rm B}$ includes contributions from both disk and bulge, and the HI is a disk property, the morphological dependence on $M_{\rm HI}/L_{\rm B}$ is complicated. Finally, the fraction of the total mass in the form of HI can be examined via the ratio $M_{\rm HI}/M_{\rm T}$. Figures 4*a–c* show the results of our analysis of HI properties.

The total HI mass $M_{\rm HI}$ is a scale parameter that is seen to vary over at least 2 orders of magnitude in the interquartile ranges and 4 orders of magnitude in the extremes. It is well know that early-type systems—E and S0 galaxies—contain proportionately lower HI masses, and in fact show a much larger range in all measures of HI content, both in $M_{\rm HI}$ and $\sigma_{\rm HI}$ relative to the later spirals. While some Es and S0s have HI contents similar to those of Sb–Sc spirals, others contain several orders of magnitude less HI. For this reason and because the HI within S0s is often located in an annulus exterior to the optical disk, van Driel & van Woerden (1991) and others have suggested that the HI gas has an external origin—the result of a tidal interaction or the infall of a dwarf companion. Bregman et al (1992) propose that almost no true Es have detectable HI gas except for those few instances where, through the HI kinematics and distribution, infall is indicated. As evident in Figure 4*c*, the fractional HI mass increases systematically from E/S0 to Im.

Among the later-type spirals, $\sigma_{\rm HI}$ is useful as an indirect probe of the effect of

local environment on star-formation potential. In the study of the HI deficiency of cluster galaxies relative to their counterparts in low density regions, Haynes et al (1984) have defined the measure of the depletion of the HI content as the difference between the observed HI mass (in logarithmic units) and that expected for a galaxy of the same linear diameter and morphological type for isolated objects. Specifically, the HI deficiency parameter is defined as

$$< DEF > = \log[M_{\rm HI}(T, D)]_o - \log[M_{\rm HI}(T, D)_{\rm obs}].$$

The use of the HI deficiency parameter has led numerous authors to conclude that spiral galaxies that pass through a hot X-ray intracluster medium are stripped of their HI gas. Haynes & Giovanelli (1986) found a one-to-one correspondence between high HI deficiency and shrunken HI size. Warmels (1988a,b) and Cayatte et al (1990) also find that the HI disks of Virgo core galaxies are indeed shrunken with respect to their field counterparts or objects outside the core. Although ram-pressure stripping is the favored explanation for the HI deficiency, analysis of the the current data do not discriminate among the alternatives of ram pressure, conductive heat transport, turbulent viscosity, or tidal effects (Magri et al 1988). In other instances, slow but close, prograde tidal encounters can similarly remove the majority of a galaxy's interstellar HI. The effect of environment is discussed further in Section 4.

Carbon Monoxide

Verter (1985, 1990) and Young & Scoville (1991) have summarized extragalactic CO observations. More recent survey results are given by Braine et al (1993), Sage (1993), and Ohta et al (1993). There is a strong correlation between FIR and CO fluxes. However, a significant fraction of the data in the literature refer to galaxies chosen by some IR criterion which in turn reflects active star formation, frequently triggered by interactions with companion galaxies. For such interacting systems Braine & Combes (1993) and Sage (1993) find a higher mass fraction of molecular hydrogen, $M_{\rm H_2}/M_{\rm T}$, than for more isolated galaxies. Sage derives a mean increase of about a factor of two. Thus some of the statistical studies have samples rich in CO because active star-forming galaxies were preferentially chosen. Reviews and conference proceedings include those by Young & Scoville (1991), Combes (1992), and Combes & Casoli (1991).

Working with a volume-limited sample Sage (1993) found that for galaxies of type Sa–Sc, $M_{\rm H_2}$ is approximately 2% of the total mass within the region where the H_2 is measured. H_2 appears to be a smaller fraction in Sd-type galaxies, significantly so if the upper limits on $M_{\rm H_2}$ in his data set are considered. To derive $M_{\rm H_2}$ Sage assumes that the conversion factor for CO to H_2 is the same in all galaxies and equal to the Galactic value. Essentially all values of $M_{\rm H_2}$ in the literature make this assumption. This appears to be a reasonable approach

for M31 and M33 but not so in later-type galaxies (Cohen et al 1988, Rubio et al 1991, Ohta et al 1993). What is evident for these late-type systems is the general faintness of the CO radiation, even though current star formation is ongoing. We must conclude that values of the molecular hydrogen content in late-type systems (Sd, Sm, Ir) derived in this manner are uncertain and possibly too low by up to an order of magnitude.

Uncertainty of a different sort also exists for CO results in early-type systems. For ellipticals there is the well recognized problem of classification uncertainty (Buta 1992a,b; Roberts et al 1991; Bregman et al 1992; Hogg et al 1993). If we wish to speak of the cool gas content in different sorts of early-type galaxies, e.g. E or S0, it is important that we minimize the classification uncertainty. Unfortunately, this is difficult and the literature is correspondingly confusing. As an example, Buta (1992a) calls attention to a well recognized Sb spiral, NGC 3928, which because of its compactness is typed as an E0 on the Palomar Sky Survey prints. This "elliptical" stands out in the *IRAS* lists and was successfully searched for CO (Gordon 1990). This is an extreme case. Generally the disagreement exists among the similar-in-appearance types of E, E/S0, S0, and Sa. But it is just in this range of galaxy type that the question is raised of bifurcation or continuity in various properties. Until quantitive measurement of type becomes possible, uncertainty will remain.

Weak CO emission has been detected in only two of over a dozen of the RSA catalog ellipticals that have been searched in depth (Sofue & Wakamatsu 1993, Roberts et al 1991, Bregman et al 1992). Only 3 (out of 64 searched) isolated RSA ellipticals have HI detections. Two of these appear to be examples of capture and the third, NGC 2974, shows spiral features on deep imaging and therefore is an Sa with low surface brightness arms. Thus cool gas, CO and HI, is a rarity in the earliest of galaxies, the ellipticals, while hot X-ray emitting gas is quite common in these systems. Cool gas is more frequently found in the early galaxies of type S0, S0/Sa, and Sa—the frequency of detection increasing in this sense. There are also instances of stringent upper limits for these galaxy types for CO and for HI. Thus, unless survival analysis which evaluates detections together with upper limits for non-detections (Feigelson & Nelson 1985) is used to derive average values of M_{H_2} and M_{HI}, trends regarding these quantities for the early-type categories will be too high.

It is both of these effects—the conversion factor for CO to H_2 for late-type galaxies and inclusion of upper limits for early-type systems—that could well alter any trend with morphological type. With this caution in mind we consider the various relationships for the molecular gas content with type [described in the review by Young & Scoville (1991)]. Those appropriate to our discussion are:

1. M_{H_2}/L_B. This ratio is essentially constant for types Sa–Sc and then decreases for later types, Scd-Sdm; the scatter is large. Using a sample selected differently, Sage (1993) found a similar trend in terms of fractional

mass content, M_{H_2}/M_T. This near constancy over Sa–Sc followed by a decrease for later types is also seen in the intrinsic quantities of radius, blue luminosity, and total mass. However, the decrease in M_{H_2}/L_B could also reflect a changing CO to H_2 conversion factor. We conclude that M_{H_2}/L_B and M_{H_2}/M_T are nearly constant over types Sa, Sb, and Sc. All we can say for later types is that the appropriately normalized CO luminosity is less.

2. M_{H_2}/M_{HI}. This ratio decreases with type S0/Sa–Sd/Sm; the scatter is large. Sage (1993) found the same trend for a different sample. He attributes it to the long recognized increase of M_{HI}/M_T with type since M_{H_2}/M_T is essentially constant (for Sa–Sc). The range and details of the M_{H_2}/M_T variation with type are obviously dependent on the conversion factor and the statistical treatment of the upper limits. He further notes, as do others (e.g. Devereux & Young 1990), the spatial anticorrelation of these two forms of hydrogen in galaxies, including our own; H_2 is more centrally concentrated than HI. We conclude that the global decrease in M_{H_2}/M_{HI} is in the expected sense and reflects the increase in M_{HI}/M_T with type.

3. $(M_{H_2} + M_{HI})$/Area. This quantity, the total cool gas surface density (note that the area is based on the optical diameter D_{25}), increases with later type. This is the sense of the trend for σ_{HI}, as well as for σ_{H_2} (Young & Knezek 1989). For the latter, constancy of σ_{H_2} over a limited mid-type range is also permissible from the data since there is the usual uncertainty at the extreme types. We conclude that the surface density of cool gas increases with later type. This is an important systematic trend, similar to that displayed by HII regions within galaxies of different type.

HII Regions

Regions of ionized hydrogen are one of the distinguishing features of galactic morphology. The first quantitative description relating galaxy type and HII regions is given by Sersic (1960) who studied their sizes as measured on broad-band photographic plates. More recently, major progress has been made by Kennicutt and his colleagues using Hα imaging in their study of nearly 100 galaxies. In a series of seminal papers (Kennicutt 1988, 1989; Kennicutt et al 1989) a census of HII region properties is given for a galaxy type range of Sa–Im. Summarized here are those that are related to morphological type. Figure 6 (taken from Kennicutt et al 1989) which shows the cumulative HII region luminosity function for galaxies of different type illustrates some of these points:

1. The brightest HII regions in late-type systems are on average ~50 times more luminous than the brightest in early-type spirals. Galaxies intermediate in type have their brightest HII regions intermediate in value, again, on average;

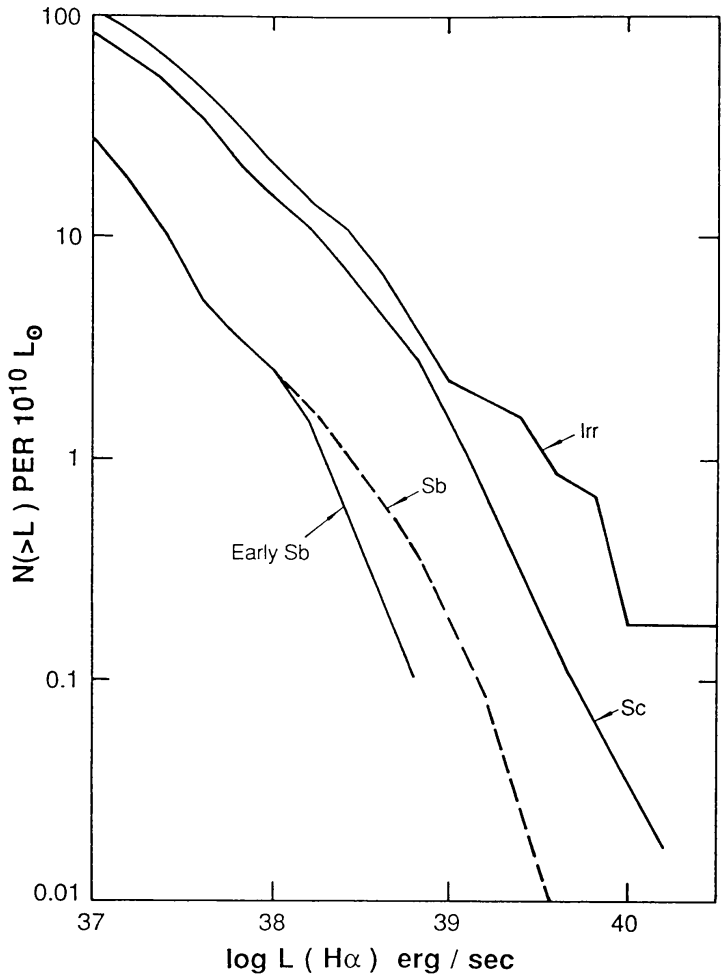

Figure 6 The cumulative HII region luminosity function for different galaxy types from Kennicutt et al (1989).

the dispersion is large. The number of bright HII regions per unit galaxy luminosity or the number expressed as a surface density varies systematically with type. Both measures are smallest for early-type spirals (Sab–Sb) and largest for Sm–Im. The difference in the mean is close to an order of magnitude. These results are for HII regions of Hα luminosity $> 10^{38}$ erg s^{-1} (and can extend to $10^{40.8}$ ergs s^{-1}). For comparison, Orion has $L(\mathrm{H}\alpha) \sim 10^{37}$ ergs s^{-1}.

2. The diameters of the first-rank HII regions vary in a similar sense: The larger ones are found in the later-type systems for galaxies of similar absolute magnitude. This luminosity normalization allows for any possible size-number effect.

3. The slope of the luminosity functions for HII regions in different galaxies shows a weak but systematic trend with type, with later-type systems hav-

ing a shallower slope. The bright end of the luminosity function shows a systematic truncation in the sense that earlier type galaxies are lacking in bright HII regions. Kennicutt et al (1989) illustrate this point by noting that 30 Dor in the LMC is ~20 times brighter than any HII region in M31, a much larger galaxy of type Sb. Furthermore the ten brightest HII regions in the LMC are all brighter than M31's brightest.

All of these trends indicate a massive star-formation rate determined by the galaxy type in which it occurs. Related to this is the systematic occurrence of the brightest stellar associations in the later-type galaxies (Wray & de Vaucouleurs 1980).

Kennicutt (1989) examined the relationship between the (disk-averaged) Hα surface brightness and the HI and CO surface density and found a threshold value for the latter, $\sim 3 M_{\odot}$ pc^{-2}, below which star formation is rare. He notes that Toomre's (1964) model for the stability of a simple single-fluid disk is consistent with these results. Hogg et al (1993) find a similar threshold value for the onset of star formation within a sample of S0s and Sas.

These results are encouraging in supporting an intuitive expectation that star formation proceeds where there is "enough" material to do so. An understanding of the next link as to why the bright end of the initial mass function varies with galaxy type will offer an important insight into massive star formation.

Chemical Abundances

Chemical abundance determinations are now of a quality and number to enable relationships with other galaxian parameters to be described. This has been done for such quantities as luminosity (Skillman et al 1989), mass (Garnett & Shields 1987, Vila-Costas & Edmunds 1992), and type. Figure 7 displays values of O/H as derived from emission line strengths measured in HII regions, as a function of type (upper panel) and of luminosity (lower panel). The trend is in the sense that the fainter, less massive, and later-type galaxies are lower in O/H.

Using absorption lines and colors, a trend for Fe/H as a function of luminosity is well described for Es and S0s, in the sense of a lower Fe value in fainter galaxies (Pagel & Edmunds 1981, Da Costa 1992). With a reasonable assumption regarding the O/H and Fe/H abundances, Skillman et al (1989) show that the spheroidals and dwarf elliptical galaxies form a smooth extension of the faint end of the abundance-luminosity relation found for spirals and irregular-type galaxies.

Intercomparison between abundances based on emission lines from HII regions and on absorption lines and colors from a stellar population is uncertain. The approaches and assumptions differ significantly (e.g. Pagel & Edmunds 1981). Atomic processes guide the emission-line analysis, while the absorption

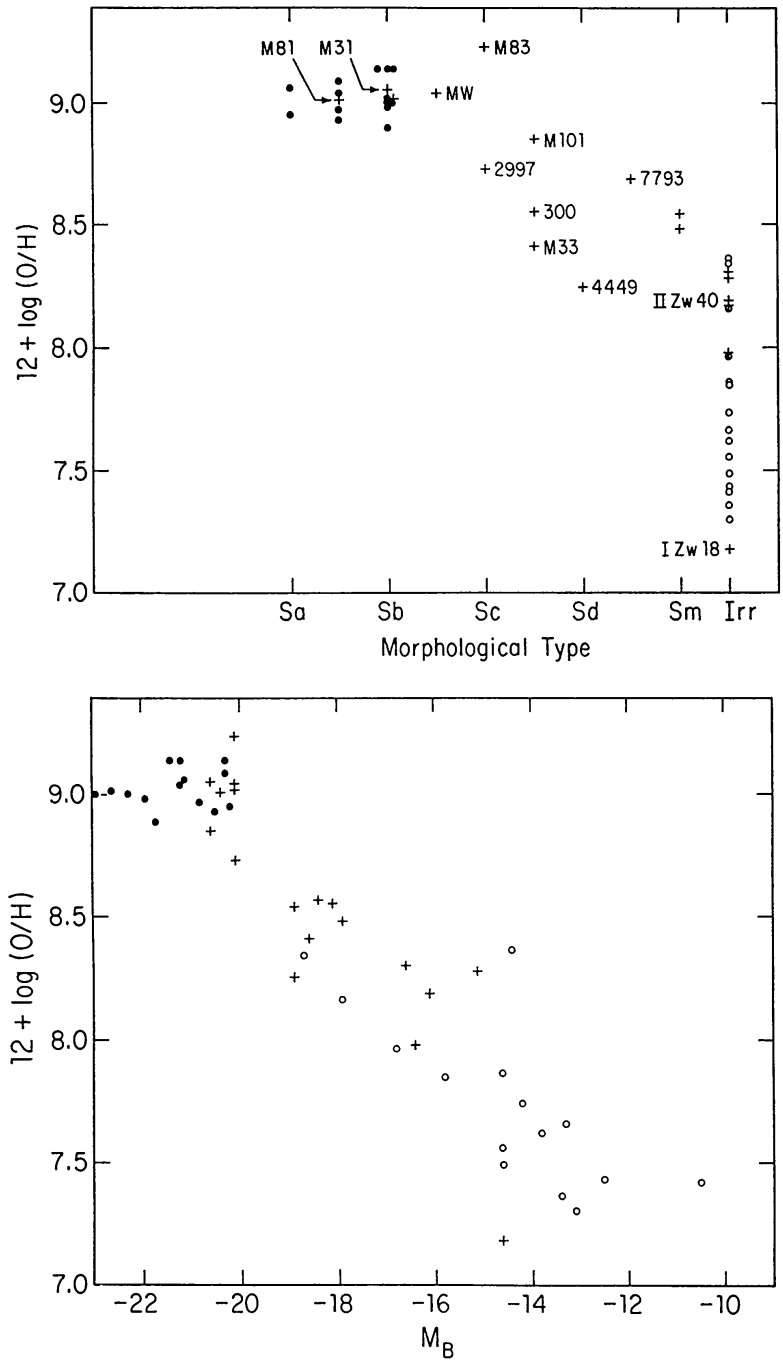

Figure 7 O/H abundance vs morphological type (*upper*) and absolute magnitude (*lower*). Different symbols represent different sources: filled circles—Oey & Kennicutt (1993), plus signs—Garnett & Shields (1987), open circles—Skillman et al (1989). The absolute magnitudes are as given in these references.

lines must be evaluated in terms of both the composite stellar population and metallicity using one of two methods: evolutionary synthesis or stellar population synthesis (e.g. Rocca-Volmerange 1992, Chiosi et al 1992, Bruzual 1992).

Even within the spiral category, where there is a systematic trend of HII region size and luminosity, the emission-line analysis can be type dependent. For early spirals, the widely used temperature indicator [O III]λ4363 line is often too weak to use. Lacking such data, an empirical method is applied in which the abundance is derived from ([OII]λ3727+ [OIII]λ5007)/Hβ and its calibration versus [O/H], a procedure which may be uncertain in the high-abundance regime. These problems and the derivation of abundances for early-type galaxies are discussed by Diaz (1992) and by Oey & Kennicutt (1993).

Although different techniques and often large uncertainties are encountered, the following consistent picture emerges:

1. The least luminous and least massive of galaxies, Ims and dEs, have the lowest abundances (O/H or Fe/H), 10^{-1} to 10^{-2} solar. The most massive and most luminous of galaxies, both ellipticals and (the central regions of) spirals are overabundant in the "heavy" elements by factors of up to a few (Strom & Strom 1978, Aaronson & Mould 1985, Worthey et al 1992). Gorgas et al (1990) suggest that, in the mean for their sample of Es and S0s, the value is near solar.

2. When measurable, most galaxies including our own show an abundance gradient in the sense of a lower metallicity at the outskirts, i.e. at larger galactocentric radii (Diaz 1992, Vila-Costas & Edmunds 1992). There appears to be a type dependence for these gradients. Early-type spirals have shallower [O/H] gradients than do late-type systems (Vila-Costas & Edmunds 1992, Oey & Kennicutt 1993). Gradients within Es and S0s show a wide range and appear not to be correlated with any galaxian parameter (Gorgas et al 1990).

3. An abundance-type effect is present among spirals and irregulars in the sense that earlier galaxies have a higher abundance. This trend reaches an approximately constant value among the early spirals. However, the entire effect may only reflect a luminosity or mass distribution in the highly selected sample of galaxies thus far studied for abundances (Garnett & Shields 1987, Skillman et al 1989, Oey & Kennicutt 1993).

There are exceptions to these various findings. Bertola et al (1993) described a metal-poor luminous early-type galaxy NGC 5018. They found that the inner region has a relatively blue color together with a weak Mg_2 index—both measures of low metallicity. Shields et al (1991) described the first sample of cluster galaxies studied for abundances. They found higher interstellar abundances in

Virgo cluster Scs than for field galaxies of similar type, which they attribute to the absence of low abundance infalling material.

A type-abundance dependence in field galaxies is present only in the broadest of terms. More fundamental may be the abundance trend with luminosity and with mass over the range from dwarf galaxy to giant (classical) galaxy.

Total Masses and Related Quantities

The study of total masses has been approached both through the measurement of global HI profile widths and through the detailed study of rotation curves. In an early work, Brosche (1971) noted that the maximum rotational velocity decreased along the spiral sequence from Sa to Im as if the morphological sequence could be understood as a sequence of angular momentum at constant mass. Today the issue appears more complicated. The masses and mass-to-light ratios of galaxies were the subject of a review by Faber & Gallagher (1979) to which the reader is referred for a general discussion.

Similarly to Faber & Gallagher, we have examined the total mass within the optical radius by using the 21 cm line width as the indicator of rotational velocity. While their analysis made use of 121 disk galaxies, the present sample contains mass estimates for over 3000 objects. Figures 2 and 3 include the distribution of properties relevant to mass: M_T, the total mass surface density σ_T, and the total mass-to-light ratio M_T/L_B.

As with luminosity and size we find, in Figure 2*c*, a small systematic variation of total mass among the classical spirals followed by a pronounced decrease for the dwarf systems. It is important to note that the three parameters L, R, and M are strongly coupled through the Tully-Fisher relations (Tully & Fisher 1977), i.e. both R and V vary with L. Unfortunately our understanding of the Tully-Fisher relations is too poor to point to the fundamental parameter(s).

TOTAL MASS-TO-LIGHT RATIO As seen in Figure 2*d*, median values of M_T/L_B are essentially constant at a value near five over the entire type range S0–Im. Although the trends of L_B, R_{lin}, and M_T are each in the same sense over this range, it still comes as a surprise to these authors to find neither a type dependence nor a distance dependence (Figure 1) in M_T/L_B. In particular, a type dependence has been found frequently in analysis of much smaller samples, though the range in slopes found in these determinations includes both positive and negative values, as well as a zero slope (Meisels 1983).

ROTATION CURVES Recent studies of the mass distribution within galaxies have employed the detailed rotation curves obtained either from the Hα or HI 21 cm line. Rubin (1991) presents a summary of the results, particularly those of the optical studies that look for environmental effects. Broeils (1992) has examined the HI rotation curves and optical surface photometry of 23 spiral and irregular galaxies to look for the morphological dependences in the distribution

of mass and light. An extensive bibliography of published rotation curves is available in Corradi & Capaccioli (1991).

In studying the dark matter distribution, HI rotation curves are more suitable since they generally extend far beyond the point where Hα is detected, and thus better constrain the halo distribution. Most recently, Broeils (1992) has combined new observations with those available in the literature to look at morphologial dependences in the mass and light distributions and the applicability of dark matter and alternative models. He sees a clear indication that the dark matter component increases for the latest types, but along the spiral sequence evidence for significant morphological trends is lacking, partly due to the still-small number of objects mapped.

With the discovery of two galaxies with declining rotation curves, Casertano & van Gorkom (1991) have found correlations between the peak circular velocity of a galaxy, its central surface brightness, and the slope of the outer rotation curve (see also Persic & Salucci 1991). As in Broeils' sample, they do not sample the full range of the spiral sequence. Kent (1987) has pointed out that Sa galaxies may require no dark matter within the optical disk, but few Sa galaxies have been mapped in HI, primarily because their lower characteristic HI surface densities make synthesis observations more difficult. The current observations suggest two conclusions:

1. Most late-type dwarf galaxies show rotation curves that are still rising at their last measured point.

2. Classical spirals show rotation curves whose outer portions are rising, flat, or falling.

MASS SURFACE DENSITY As evident in Figure 3*c*, the total mass surface density σ_T shows a clear decrease along the spiral sequence. The trend is slow but monotonic from S0/a to Sc with a steepening toward the dwarfs.

4. VARIATIONS IN GALAXY PROPERTIES

Some of the systematics in the properties of galaxies point to a common thread—that of star formation. In this section, we investigate trends along the Hubble sequence and consider also the critical parameter of local environment.

Global Properties

We have discussed 18 measures of the properties of galaxies. For five of these there is a clear monotonic variation with morphological type over the entire spiral-irregular range. A sixth, that of the luminosity function of HII regions, also shows such a monotonic type-dependent variation, though here the data are far fewer. All six are normalized quantities, i.e. the "size" of the system

is allowed for: σ_T, σ_{HI}, M_{HI}/L_B, M_{HI}/M_T, (B − V), and HII region luminosity functions. However not all of the normalized (nor absolute) quantites vary systematically and monotonically, e.g. M_T/L_B, Σ_B, σ_{FIR}. Five of the six can be identified with star-formation activity: past, present, or future potential. The sixth, the mass surface density, is also likely related to such activity as a triggering mechanism. Thus, (B − V) measures past and current formation activity, HII regions relate current activity, and the cool gas content measures the reservoir for future star formation. In addition, those parameters for which the data are too few to describe any detailed type dependence other than elliptical versus spiral—radio, X-ray, and chemical abundance—are also star formation related. What is surprisingly lacking from this overall list is the FIR surface density. It does have the elliptical vs spiral dependence of others but shows no variation within the classical spiral category (and only an uncertain trend in the later types due to fewer data). This lends support to the two-component model for the origin of the FIR described previously. Clearly, the morphological sequence of normal, isolated galaxies measures star-formation activity.

The Effect of Environment

Perhaps the strongest differences among galaxies of different morphologies are seen in their clustering tendencies. In individual cases, the importance of mergers, tidal interactions, and sweeping within clusters can readily be demonstrated, yet the overall imprint of recent processes on galaxy morphology remains unclear. Below, we review the evidence for morphological segregation and the importance of interactions between galaxies and their surroundings.

MORPHOLOGICAL SEGREGATION As early as the 1880s, Wolf noticed that the distribution of nebulae was not uniform in the sense that more elliptical nebulae were concentrated in the Virgo direction than elsewhere. By the 1930s, the morphological differences between field and cluster galaxies were well established (Hubble & Humason 1931). Using his survey of 55 rich clusters, Dressler (1980) has quantified the concept of morphological segregation, showing the steady decrease in spiral fraction and the corresponding increase in the E/S0 population with local galaxy density, a variation in population fraction that is slow but monotonic. Extending Dressler's study, Postman & Geller (1984) have shown that the morphology-density relation holds over six orders of magnitude in space density to regimes where the dynamical timescale approaches the Hubble time.

THE CLUSTER ENVIRONMENT In the highest density environments, the possible morphology-altering mechanisms are many; galaxy-galaxy, galaxy-cluster, and galaxy-intracluster medium interactions can all lead to significant changes in morphology and star-formation potential. Indeed, the occurrence of patholog-

ical and disturbed objects in high density regions is well-recognized. Dressler (1984) reviews the models for morphological alteration in clusters according to the relative importance of initial conditions or late evolution. Whitmore (1990) gives a recent summary of the various galaxy properties that are seen to vary significantly between cluster and field galaxies.

In addition to the obvious variation in morphological make-up, various authors have attempted to identify density dependences in the fundamental properties under consideration in this review. It has already been mentioned in Section 3 that spiral galaxies passing through the center of rich X-ray clusters appear to lose up to 90% of their interstellar HI. At the same time, their molecular consitutents, as measured by their CO content and distribution, remain relatively unaffected (Kenney & Young 1989). Evidence for the stripping of spirals in clusters and constraints on the responsible processes are reviewed in Haynes (1990).

Most recently, studies have addressed the possibility of environmental variations in the distribution of mass within galaxies, and the results are conflicting. The detailed studies of rotation curves of spiral galaxies in clusters by Rubin et al (1988) and Whitmore et al (1988) suggest that, in inner cluster members, the halo is either partially stripped or not allowed to form—a conclusion based on the observation of falling rotation curves in centrally located galaxies. However, Distefano et al (1990), using Hα rotation curves, and Guhathakurta et al (1988), using ones derived from HI synthesis maps, do not see such environmental effects in their respective studies of Virgo members.

THE GROUP ENVIRONMENT In loose groups, where the velocity dispersion is low, slow close prograde tidal encounters can remove significant fractions of a galaxy's interstellar material. A classic, graphical discussion of the tidal phenomenon is given by Toomre & Toomre (1972), and numerous examples of the success of these models in reproducing tidal bridges and tails are now available. Both radio emission and far infrared emission are strongly enhanced in the instance of tidal interactions. The importance of interactions in a wide range of phenomena from the formation of shells and polar rings to the driving of spiral stucture and starburst phenomena have been discussed by numerous authors, most recently Barnes & Hernquist (1992).

GALAXIES AT HIGH REDSHIFT Evidence is now accumulating that significant evolution of the cluster population has occured between the present time and the epoch corresponding to a redshift $z \simeq 0.4$ (for a review see Koo & Kron 1992). Clusters in the range $0.4 \leq z \leq 1$ show a higher fraction of blue galaxies than do their low redshift counterparts, the so-called Butcher-Oemler effect. Gunn (1990) reviews the evidence for the Butcher-Oemler effect including the increase in emission-line and Seyfert objects and the presence of the "E + A" population. Recent high resolution imaging of the blue cluster members confirms their spiral nature (Lavery et al 1992, Dressler & Gunn 1992). The re-

lationship of the present-day population to the distant cluster galaxies and their field counterparts is critical to our understanding of the process of galaxy evolution and the development of the morphological characteristics evident today.

The S0 Problem

For the most part in this review, we have not emphasized the importance of the S0 class. If a spiral loses 90% of its interstellar HI, its potential for future star formation must be greatly diminished and thus its spiral structure should fade (Larson et al 1980). The resultant object would look like an S0. As pointed out by Giovanelli & Haynes (1985), the S0 fraction at a given density in Dressler's (1980) survey is higher in X-ray luminous clusters, while the corresponding spiral fraction is lower. At the same time though, fundamental differences in the bulge to disk ration and in surface magnitude still distinguish the S0 galaxies from present-day spirals (Dressler 1980). Whereas one fifth of the S0s in the RSA contain significant amounts of HI, others of similar properties are lacking in HI to much lower limits (Bregman et al 1992). The HI detection rate is so much higher than that for ellipticals that a capture hypothesis is unlikely. Pogge & Eskridge (1993) found a similar dichotomy in the presence of HII regions in S0 disks, but concluded that the S0s merely represent the early-type end of a continous variation in star-formation activity along the spiral sequence. Because of the large dispersion in properties, the S0 class still remains enigmatic.

Classical Galaxies vs Dwarfs

We concur with, among others Sandage et al (1985) and Binggeli (1993), that there are fundamental differences between bright ("classical") and faint ("dwarf") galaxies. The RC3 contains too few dEs for an interpretation of their characteristics in our analysis, but repeatedly in Figures 2 and 3 and Table 1, clear distinctions are seen in the latest types. Sandage (1990) summarizes the results of the Las Campanas surveys of the Virgo and Fornax clusters and selected loose groups conducted by him and his collaborators. In particular, these studies have explored the relative distributions of dE and Im dwarfs. They conclude that:

1. Dwarf galaxies have the same general space distribution as giant galaxies. The dEs are predominantly found in dense groups whereas the Ims are more widely dispersed. The dEs at least seem to form only in the vicinity of more massive galaxies.

2. The faint end slope of the luminosity function for dEs in the field is flatter than that found for similar galaxies in Virgo or Fornax.

3. The dwarf to classical ("giant") galaxy ratio decreases in low richness regions relative to ratios found in clusters.

5. SUMMARY

In this review we have discussed quantifiable properties of galaxies and their dependence on morphological type. Why the present-day galaxy population follows these trends is a major challenge of theories of galaxy formation and evolution. Here, we conclude with the following summary of the behavior of the "typical" galaxies found in today's large catalogs:

1. There are *three* general categories of galaxies: elliptical, classical spiral, and dwarf. This last category includes Sd and Sm. The nature of S0s remains a matter of debate, perhaps because they are indeed a transition type.

2. There is a pronounced spatial segregation of morphologies in the sense that early-type galaxies are more clustered.

3. For a volume-limited sample, we find that the classical spirals—Sa, Sb, Sc—show a small systematic variation in median size and in median luminosity, becoming larger and brighter as they become later. There is a suggestion of a similar trend for total mass. We do not find these dependences in the flux-limited sample.

4. The late-type dwarfs are indeed different from the classical galaxies. The dwarfs become smaller, fainter, and less massive over the range Scd–Im.

5. The mass-to-luminosity ratio is essentially constant over the entire sequence S0–Im. Although this ratio is distance dependent, it shows essentially no Malmquist bias.

6. The total mass surface density σ_T decreases systematically over the sequence S0/a–Im.

7. There are a number of systematic trends with type in these data that are clearly identifiable with star-formation processes. Thus global color is a measure of past and present star-formation activity, as are X-ray and radio radiation. The HII region parameters relate to current activity; the cool gas components measure the potential for future star formation. The trend of abundances is also consistent with the above picture but FIR measurements are not.

8. We must stress the wide range to be found for any parameter within any type. The range is always larger than even the most pessimistic error estimates. Much of this wide range is intrinsic. The only instance where overlap does not occur at least over the interquartile interval is for Ims vs classical spirals for the three basic parameters of $R_{\rm lin}$, $L_{\rm B}$, and $M_{\rm T}$.

9. The wide range in any of the parameters described above must not be interpreted to mean that parameter space is unbounded. There is an upper limit to $L_{\rm B}$ as displayed in Figure 1. But, similarly, there are lower bounds to at least the classical spirals. In particular, there are no very faint or very small Sb galaxies.

In such a summary it seems worthwhile to restate the morphological distinctions for the sequence elliptical–classical spiral–dwarf. The sequence is one of bulge-to-disk ratio, largest for the ellipticals and zero for the dwarfs. It also follows the development of spiral arms, ending with what might be thought of as a limiting case, an Im as just an arm.

ACKNOWLEDGMENTS

We thank Riccardo Giovanelli for his collaboration in developing the database used herein and both he and David Hogg for many discussions relevant to our review. Thanks are also given to Harold Corwin for suppling us with a digital copy of the RC3 and to Fran Verter, Trinh Thuan, Jim Condon, and Joel Bregman for answering inquiries and supplying data. M. P. H. receives support through NSF grants AST-9014850 and AST-9023450.

Table 1 Statistical properties of the morphological classes

	Sample		E,S0	S0a,Sa	Sab,Sb	Sbc,Sc	Scd,Sd	Sm,Im
R_{lin} (kpc)	UGC	median	21.1	19.8	25.1	22.4	17.7	8.5
		25%	14.0	13.9	18.4	16.4	11.8	4.9
		75%	28.8	26.5	32.1	29.8	24.0	14.0
		Number	1363	798	1488	1139	2223	919
	LSc	median	9.0	9.8	12.0	13.2	9.3	6.0
		25%	5.8	6.9	8.3	9.5	6.8	4.1
		75%	13.2	13.6	16.7	17.7	12.2	8.3
		Number	705	342	454	616	1037	958
L_B (10^9 $L_\odot$)	UGC	median	52.5	43.6	69.2	52.5	25.7	2.7
		25%	21.4	21.4	38.0	29.5	9.8	1.0
		75%	93.3	79.4	107.2	95.5	53.7	7.1
		Number	1302	761	1391	1029	1527	416
	LSc	median	11.0	13.2	19.5	21.9	6.8	1.9
		25%	4.2	5.4	8.1	9.3	3.2	0.8
		75%	24.0	23.4	38.0	41.7	13.2	4.1
		Number	665	315	407	563	834	595
M_T (10^{10} $M_\odot$)	UGC	median		22.6	32.4	19.0	7.9	1.6
		25%		8.7	17.0	9.5	3.5	0.5
		75%		49.0	52.5	33.9	16.6	4.0
		Number		292	808	639	1471	490
	LSc	median		7.1	11.0	9.1	2.8	1.0
		25%		3.2	4.9	5.1	1.4	0.4
		75%		17.4	21.4	16.2	5.1	1.8
		Number		119	251	389	701	534
M_T/L_B ($M_\odot/L_\odot$)	UGC	median		4.9	4.4	3.8	3.5	4.2
		25%		3.1	3.2	2.9	2.6	2.6
		75%		7.2	6.0	5.4	5.0	6.8
		Number		278	749	567	1025	245
	LSc	median		5.1	5.0	4.2	4.1	5.0
		25%		3.1	3.4	3.2	3.0	3.1
		75%		8.8	6.9	6.0	6.0	7.9
		Number		112	238	362	574	342

Table 1 Statistical properties of the morphological classes (*cont.*)

	Sample		E,S0	S0a,Sa	Sab,Sb	Sbc,Sc	Scd,Sd	Sm,Im
Σ_B	UGC	median	14.20	13.98	13.96	14.00	14:02	14.59
		25%	13.82	13.47	13.44	13.44	13.29	14.08
		75%	14.62	14.39	14.41	14.48	14.63	15.23
		Number	1591	977	1694	1154	1663	457
	LSc	median	13.78	13.73	13.55	13.72	14.02	14.73
		25%	13.51	13.36	13.10	13.23	13.39	14.21
		75%	14.15	14.10	13.99	14.22	14.65	15.35
		Number	682	317	412	571	858	649
σ_T ($M_\odot pc^{-2}$)	UGC	median		188.9	154.7	124.2	91.4	74.5
		25%		133.4	115.2	94.5	67.8	49.2
		75%		249.8	199.9	167.6	119.6	113.2
		Number		292	808	639	1471	490
	LSc	median		200.8	178.2	148.5	95.8	81.4
		25%		121.7	125.4	108.1	69.6	52.1
		75%		323.1	242.8	194.2	131.8	120.0
		Number		119	251	389	701	534
σ_{HI} ($M_\odot pc^{-2}$)	UGC	median	1.31	4.64	7.70	9.83	9.80	10.85
		25%	0.33	2.12	4.62	6.92	6.93	6.86
		75%	4.93	9.12	11.39	14.00	13.82	16.71
		Number	403	535	1200	1053	2106	902
		Detect	217	450	1149	1031	2071	894
	LSc	median	1.40	4.45	7.95	10.84	10.82	12.09
		25%	0.26	1.25	4.48	7.20	7.39	7.51
		75%	5.81	11.11	13.86	16.36	16.04	19.23
		Number	288	212	349	561	967	906
		Detect	146	178	340	557	963	901
σ_{FIR} ($L_\odot pc^{-2}$)	UGC	median	3.77	11.47	9.22	6.73	3.63	7.44
		25%	1.00	3.32	4.23	3.21	1.84	3.07
		75%	13.15	28.45	18.85	14.14	8.07	22.88
		Number	256	271	684	698	887	90
		Detect	127	205	549	517	439	73
	LSc	median	1.41	5.98	7.44	7.54	2.49	4.93
		25%	0.51	1.78	3.06	3.04	1.03	2.26
		75%	4.64	20.21	16.02	18.48	5.83	17.33
		Number	151	108	167	211	283	60
		Detect	58	83	145	191	172	48

Table 1 Statistical properties of the morphological classes (*cont.*)

	Sample		E,S0	S0a,Sa	Sab,Sb	Sbc,Sc	Scd,Sd	Sm,Im
M_{HI}	UGC	median	1.24	5.62	15.14	15.85	9.33	2.40
(10^9 $M_\odot$)		25%	0.23	1.78	6.92	7.94	4.07	0.74
		75%	5.01	13.49	26.30	26.30	17.78	6.17
		Number	410	537	1204	1058	2121	942
		Detect	222	452	1153	1036	2086	934
	LSc	median	0.52	1.41	4.17	5.89	3.02	1.27
		25%	0.10	0.42	1.67	3.02	1.41	0.43
		75%	1.58	4.36	8.71	12.59	5.76	2.69
		Number	295	213	354	567	987	974
		Detect	153	179	345	563	983	969
M_{HI}/L_B	UGC	median	0.04	0.12	0.21	0.29	0.36	0.66
($M_\odot/L_\odot$)		25%	0.01	0.04	0.12	0.19	0.24	0.36
		75%	0.12	0.24	0.33	0.43	0.56	1.10
		Number	394	510	1126	955	1444	406
		Detect	207	425	1075	934	1424	399
	LSc	median	0.03	0.10	0.20	0.30	0.47	0.78
		25%	0.01	0.03	0.11	0.18	0.28	0.44
		75%	0.14	0.28	0.34	0.48	0.76	1.32
		Number	283	201	325	513	780	555
		Detect	141	167	316	509	776	551
M_{HI}/M_T	UGC	median		0.03	0.05	0.08	0.11	0.15
		25%		0.02	0.03	0.05	0.08	0.09
		75%		0.06	0.09	0.12	0.15	0.23
		Number		292	808	639	1471	490
	LSc	median		0.03	0.04	0.07	0.11	0.15
		25%		0.10	0.02	0.04	0.07	0.09
		75%		0.07	0.08	0.11	0.16	0.24
		Number		119	251	389	700	534
L_{FIR}	UGC	median	1.71	9.89	14.26	9.87	4.05	1.63
(10^9 $L_\odot$)		25%	0.33	2.41	5.78	4.35	1.53	0.27
		75%	12.07	25.40	30.15	21.92	9.72	10.63
		Number	263	272	688	701	893	95
		Detect	131	205	553	519	442	78
	LSc	median	0.40	1.96	3.74	4.84	0.78	0.55
		25%	0.15	0.75	1.27	1.51	0.34	0.17
		75%	0.90	3.98	7.88	11.52	2.16	1.83
		Number	155	108	171	214	289	69
		Detect	59	83	149	193	175	53

Table 1 Statistical properties of the morphological classes (*cont.*)

	Sample		E,S0	S0a,Sa	Sab,Sb	Sbc,Sc	Scd,Sd	Sm,Im
(B–V)	UGC	median	0.90	0.78	0.64	0.55	0.48	0.42
		25%	0.86	0.66	0.55	0.47	0.42	0.35
		75%	0.94	0.83	0.73	0.62	0.57	0.53
		Number	484	161	243	320	161	168
	LSc	median	0.89	0.78	0.62	0.52	0.48	0.42
		25%	0.84	0.65	0.55	0.44	0.42	0.35
		75%	0.92	0.84	0.71	0.59	0.56	0.51
		Number	421	156	182	282	180	210

Literature Cited

Aaronson M, Mould J. 1985. *Ap. J.* 290:191

Barbuy B, Renzini A., eds. 1992. *Proc. IAU Symp. 149.* Dordrecht:Kluwer

Barnes JE, Hernquist LE. 1992. *Annu. Rev. Astron. Astrophys.* 30:705

Bertola F, Burstein D, Buson LM. 1993. *Ap. J.* 403:573

Binggeli B. 1993. In *Panchromatic View of Galaxies.* In press

Binggeli B, Sandage A, Tammann GA. 1985. *Astron. J.* 90:1681

Binggeli B, Sandage A, Tammann GA. 1988. *Annu. Rev. Astron. Astrophys.* 26:509

Bothun GD, Lonsdale CJ, Rice W. 1989. *Ap. J.* 341:129

Bottinelli L, Gouguenheim L. 1974. *Astron. Astrophys.* 36:461

Braine J, Combes F. 1993. *Astron. Astrophys.* 269:7

Braine J, Combes F, Casoli F, Dupraz C, Gerin M, et al. 1993. *Astron. Astrophys.*S 97:887

Bregman JN, Hogg DE, Roberts MS. 1992. *Ap. J.* 387:484

Broeils AH. 1992. *Dark and Visible Matter in Spiral Galaxies.* PhD thesis. Univ. Groningen

Brosche P. 1971. *Astron. Astrophys.* 13:293

Bruzual G. 1992. See Barbuy & Renzini 1992, p. 311

Buat V, Deharveng JM. 1988. *Astron. Astrophys.* 195:60

Burstein D, Haynes MP, Faber S. 1991. *Nature* 353:515

Buta R. 1992a. In *Morphological and Physical Classification of Galaxies,* ed. G Longo, M Capaccioli, G Busarello, p. 1. Dordrecht:Kluwer

Buta R. 1992b. See Thuan et al 1992, p. 3

Byun Y. 1993. *Publ. Astron. Soc. Pac.* 105:993

Canizares CR, Fabbiano G, Trinchieri G. 1987. *Ap. J.* 312:503

Casertano S, van Gorkom JH. 1991. *Astron. J.* 101:1231

Cayatte V, van Gorkom JH, Balkowski C, Kotanyi C. 1990. *Astron. J.* 100:604

Chiosi C, Bertelli G, Bressan A. 1992. See Barbuy & Renzini 1992, p. 321

Cohen RS, Dame TM, Garay G Montani J, Rubio M, Thaddeus P. 1988. *Ap. J.*L 331:L95

Combes F. 1992. See Thuan et al 1992, p. 35

Combes F, Casoli F., eds. 1991. *Proc. IAU Symp. 146.* Dordrecht:Kluwer

Condon JJ. 1992 *Annu. Rev. Astron. Astrophys.* 30:575

Condon JJ, Broderick JJ. 1988. *Astron. J.* 96:30

Condon JJ, Frayer DT, Broderick JJ. 1991. *Astron. J.* 101:362

Corradi RLM, Capaccioli M. 1991. *Astron. Astrophys.* 90:121

Cox P, Mezger PG. 1989. *Astron. Astrophys. Rev.* 1:49

Da Costa GS. 1992. See Barbuy & Penzini 1992, p. 191

de Jong T, Clegg PE, Soifer BT, Rowan-Robinson M, et al. 1984. *Ap. J.*L 278:L67

de Vaucouleurs G. 1959. In *Handbuch der Physik,* Vol. 53, ed. S. Flugge, p. 275. Berlin:Springer-Verlag

de Vaucouleurs G, de Vaucouleurs A, Corwin HG, Buta RJ, Paturel G, Fouque P. 1991. *Third Reference Catalogue of Bright Galaxies.* New York:Springer-Verlag

Devereux NA, Eales SA. 1989. *Ap. J.* 340:708

Devereux NA, Young JS. 1990. *Ap. J.* 359:42
Devereux NA, Young JS. 1991. *Ap. J.* 371:515
Devereux NA, Young JS. 1992. *Astron. J.* 103:1536
Diaz AI. 1992. In *Evolutionary Phenomena In Galaixes,* ed. JE Beckman, BEJ Pagel, p. 377. Cambridge:Cambridge Univ. Press
Disney M, Davis J, Phillipps S. 1989. *MNRAS* 239:939
Disney M, Phillips S. 1983. *MNRAS* 205:1253
Distefano A, Rampazzo R, Chincarini G, de Souza R. 1990. *Astron. Astrophys.* S 86:7
Dressler A. 1980. *Ap. J.* 236:351
Dressler A. 1984. *Annu. Rev. Astron. Astrophys.* 22:185
Dressler A, Gunn JE. 1992. *Ap. J.* S 78:1
Fabbiano G. 1989. *Annu. Rev. Astron. Astrophys.* 27:87
Fabbiano G, Gioia IM, Trinchieri G. 1988. *Ap. J.* 324:749
Fabbiano G, Kim D-W., Trinchieri G. 1992. *Ap. J.* S 80:531
Faber SM, Gallagher J. 1979. *Annu. Rev. Astron. Astrophys.* 17:135
Feigelson ED, Nelson PI. 1985. *Ap. J.* 293:192
Fitt AJ, Alexander P, Cox MJ. 1988. *MNRAS* 233:907
Freeman KC. 1970. *Ap. J.* 160:811
Garnett DR, Shields GA. 1987. *Ap. J.* 317:82
Gilmore G, Hodge P, van der Kruit PC. 1990. *The Milky Way as a Galaxy,* Mill Valley:Univ. Sci. Books
Gilmore G, Roberts MS. 1988. *Comments Astrophys.* 12:123
Giovanelli R, Haynes MP. 1985. *Ap. J.* 292:404
Giovanelli R, Haynes MP. 1990. In *Galactic and Extragalactic Radio Astronomy,* ed. GL Verschuur, KI Kellermann, p. 522. Berlin:Springer-Verlag
Giovanelli R, Haynes MP, Salzer JJ, Wegner G, da Costa LN, Freudling W. 1994. *Astron. J.* In press
Giovanelli R, Haynes MP. 1991. *Annu. Rev. Astron. Astrophys.* 29:499
Gizis JE, Mould JR, Djorgovski S. 1993. *Publ. Astron. Soc. Poc.* 105:871
Gordon MA. 1990. *Ap. J.* L 350:L29
Gorgas J, Efstathiou G, Salamanca A. 1990. *MNRAS* 245:217
Guhathakurta P, van Gorkom JH, Kotanyi CG, Balkowski C. 1988. *Astron. J.* 96:851
Gunn JE. 1990. See Oegerle et al 1990, p. 341
Haynes MP. 1990. See Oegerle et al 1990, p. 177
Haynes MP, Giovanelli R. 1986. *Ap. J.* 306:466
Haynes MP, Giovanelli R, Chincarini GL. 1984. *Annu. Rev. Astron. Astrophys.* 22:445
Haynes MP, Herter T. 1988. *Astron. J.* 96:504
Hewitt J, Haynes MP, Giovanelli R. 1983. *Astron. J.* 88:272
Hogg DE, Roberts MS, Sandage A. 1993. *Astron. J.* 106:907
Holmberg E. 1958. *Medd. Lund. Ast. Obs.* Ser. II, No. 136
Hubble E. 1926. *Ap. J.* 64:321
Hubble E. 1936. *The Realm of the Nebulae.* New Haven:Yale Univ. Press
Hubble E, Humason M. 1931. *Ap. J.* 74:43
Hummel E. 1990. In *Windows on Galaxies,* ed. G Fabbiano, JS Gallagher, A Renzini, p. 141. Dordrecht:Kluwer
Hummel E, van der Hulst JM, Dickey JM. 1984. *Astron. Astrophys.* 134:207
Kenney J, Young JS. 1989. *Ap. J.* 344:171
Kennicutt RC. 1988. *Ap. J.* 334:144
Kennicutt RC. 1989. *Ap. J.* 344:685
Kennicutt RC. 1990. In *The Interstellar Medium in Galaxies,* ed. HA Thronson, JM Shull, p. 405. Dordrecht:Kluwer
Kennicutt RC, Edgar BK, Hodge PW. 1989. *Ap. J.* 337:761
Kent S. 1987. *Astron. J.* 93:816
Koo DC, Kron RG. 1992. *Annu. Rev. Astron. Astrophys.* 30:613
Larson RB, Tinsley BM, Caldwell N. 1980. *Ap. J.* 237:692
Lavery RJ, Pierce MJ, McClure RD. 1992. *Astron. J.* 104:2067
Lonsdale Persson CJ, Helou G. 1987. *Ap. J.* 314:513
Magri C, Haynes MP, Forman W, Jones C, Giovanelli R. 1988. *Ap. J.* 333:136
Meisels A. 1983. *Astron. Astrophys.* 118:21
Nilson P. 1973. *Uppsala General Catalogue of Galaxies,* Acta Univ. Ups. Ser. V:A, Vol. 1, Uppsala
Oegerle WR, Fitchett MJ, Danly L, eds. 1990. *Clusters of Galaxies.* New York:Cambridge Univ. Press
Oey MS, Kennicutt RC. 1993. *Ap. J.* 411:137
Ohta K, Tomita A, Saito M, Sasaki M, Nakai N. 1993. *Publ. Astron. Soc. Japan.* 45:L21
Pagel BEJ, Edmunds MG. 1981. *Annu. Rev. Astron. Astrophys.* 19:77
Persic M, Salucci P. 1991. *Ap. J.* 368:60
Pogge RW, Eskridge PB. 1993. *Astron. J.* 106:1405
Postman M, Geller M. 1984. *Ap. J.* 281:95
Roberts MS. 1969. *Astron. J.* 74:859
Roberts MS, Hogg DE, Bregman JN, Forman WR, Jones G. 1991. *Ap. J.* S 75:751
Rocca-Volmerange B. 1992. See Barbuy & Renzini, 1992. p. 357
Rowan-Robinson M. 1990. In *The Interstellar Medium in Galaxies,* ed. HA Thronson, JM Shull, p. 121. Dordrecht:Kluwer
Rubin VC. 1991. In *After the First Three Minutes,* ed. SS Holt, CL Bennett, V Trimble, p. 371. New York:Am. Inst. Phys.
Rubin VC, Whitmore BC, Ford WK Jr. 1988. *Ap. J.* 333:522
Rubio M Garay G, Montani J, Thaddeus P. 1991. *Ap. J.* 368:173
Sage LJ. 1993. *Astron. Astrophys.* 272:123
Sandage A. 1961. *The Hubble Atlas of Galaxies,* Washington:Carnegie Inst. Washington

Sandage A. 1975. In *Stars and Stellar Systems,* Vol. 9, ed. A Sandage, M Sandage, J Kristian, p. 1. Chicago:Univ. Chicago Press
Sandage A. 1990. See Oegerle et al 1990, p. 201
Sandage A, Bedke J. 1993. *Carnegie Atlas of Galaxies,,* Washington:Carnegie Inst. Washington. In press
Sandage A, Binggeli B, Tammann GA. 1985. *Astron. J.* 90:1759
Sandage A, Tammann GA. 1987. *A Revised Shapley-Ames Catalog of Bright Galaxies.* Washington:Carnegie Inst. Washington
Sanders DB, Soifer BT, Neugebauer G, Scoville N, Madore BF, et al. 1987. In *Star Formation in Galaxies,* ed. CJ Lonsdale Persson, p. 411. Washington:NASA
Sarazin CL. 1992. See Thuan et al 1992, p. 51
Sauvage M, Thuan TX. 1992. *Ap. J.*L 396:L69
Sauvage M, Thuan TX. 1993. *Ap. J.* In press
Scalo JM. 1986. *Fund. Cosmic Phys.* 11:1
Schechter P. 1980. *Astron. J.* 85:801
Sersic JL. 1960. *Z. Astrophys.* 50:168
Shields GA, Skillman ED, Kennicutt RC. 1991. *Ap. J.* 371:82
Skillman ED, Kennicutt RC, Hodge PW. 1989. *Ap. J.* 347:875
Sofue Y, Wakamatsu K. 1993. *Publ. Astron. Soc. Jpn.* 45:529
Soifer BT, Houck JR, Neugebauer G. 1987. *Annu. Rev. Astron. Astrophys.* 25:187
Strom KM, Strom SE. 1978. *Astron. J.* 83:73
Telesco CM. 1988. *Annu. Rev. Astron. Astrophys.* 26:343
Thuan TX, Balkowski C, Van JTT, eds. 1992. *Physics of Nearby Galaxies.* Gif-sur-Yvette: Frontiers
Toomre A. 1964 *Ap. J.* 139:1217
Toomre A, Toomre J. 1972. *Ap. J.* 178:623
Tully RB, Fisher JR. 1977. *Astron. Astrophys.* 54:661
Valentijn E. 1991, *Nature* 346:153
van Driel W, van Woerden H. 1991. *Astron. Astrophys.* 243:71
Verter F. 1985 *Ap. J.* S 57:261
Verter F. 1990 *Publ. Astron. Soc. Pac.* 102:1281
Vila-Costas MB, Edmunds MG. 1992. *MNRAS* 259:121
Warmels RH. 1988a. *Astron. Astrophys.*S 72:19
Warmels RH. 1988b. *Astron. Astrophys.*S 72:57
Watanabe M, Kodaira K, Okamura S. 1985. *Ap. J.* 292:72
Whitmore, B. 1984. *Ap. J.* 278:61
Whitmore B. 1990. See Oegerle et al 1990, p. 139
Whitmore BC, Forbes DA, Rubin VC. 1988. *Ap. J.* 333:542
Whitmore BC, McElroy DB, Tonry JL. 1985. *Ap. J.* S 59:1
Worthy G, Faber S, Gonzalez J. 1992. *Ap. J.* 398:69
Wray JD, de Vaucouleurs G. 1980 *Astron. J.* 85:1
Xu C. 1990 *Ap. J.* L 365:L47
Young JS, Knezek PM. 1989. *Ap. J.* L 347:L55
Young JS, Scoville NZ. 1991. *Annu. Rev. Astron. Astrophys.* 29:581
Zwicky F. 1957. *Morphological Astronomy.* Berlin:Springer-Verlag